Distributionally Robust Chance Constrained Optimization for Providing Flexibility in an Active Distribution Network

Mohammad Rayati, Mokhtar Bozorg, *Member, IEEE*, Rachid Cherkaoui, and Mauro Carpita, *Member, IEEE*

***Abstract*—In this paper, we propose a distributionally robust chance constrained (DRCC) optimization problem for the operation of an active distribution network (ADN). The ADN's operator uses the proposed problem to centrally optimize the dispatch plan of his resources, namely photovoltaic (PV) and battery energy storage (BES) systems, and to participate in wholesale real/reactive power and flexibility markets. We model the uncertainties in the problem by knowing a set of probability distributions, i.e., *an ambiguity set*. The uncertainties include production capability of PV systems, end-users' consumption, requested flexibility by the external network's operator, and voltage magnitude at the point of common coupling (PCC). The resulting formulation is a DRCC optimization problem for which a solution methodology based on freely available solvers is presented. We evaluate the performance of proposed solution in the numerical results section by comparing it with two benchmark models based on stochastic and chance constrained (CC) optimization.**

***Index Terms*—Active distribution network (ADN), battery energy storage (BES) systems, distributionally robust chance constrained (DRCC) optimization, flexibility, photovoltaic (PV) systems.**

I. Introduction

A. Context and Literature Review

THE SUPPORT of distributed resources in active distribution networks (ADNs) for providing flexibility is an essential asset for the system operator to accommodate high penetration of renewable energy sources in tomorrow's electrical networks [1]. Here, we refer to distributed resources such as photovoltaic (PV) and battery energy storage (BES) systems. In addition, flexibility refers to the ability of regulating real/reactive power profiles of the distributed resources and, subsequently, at the point of common coupling (PCC).

Due to the small size and large number of distributed resources that provide flexibility, we cannot incorporate the decision variables of distributed resources directly into large-scale problems of electrical networks, e.g., wholesale markets. Each ADN's operator is responsible for ensuring that the dispatch plan of distributed resources with planned/requested flexibility at the PCC complies with the operational constraints and uncertainties of the ADN. In this regard, we obtain the optimal dispatch plan for the PV and BES systems by considering the operational constraints and uncertainties for planning and providing flexibility in an ADN.

In [2], an optimal dispatch plan for an ADN has been proposed, ignoring the network's uncertainties and physical constraints. The dispatch plan of an ADN has been determined using a hybrid of stochastic and robust optimization, according to [3]. A *two-stage* framework for dispatching the power of an ADN has been developed in [4], with a BES system serving as a flexible element. The dispatch plan, including the power profile that we must realize at the PCC during the operation, has been determined in the *first-stage*, allowing the BES system to regain an adequate level of flexibility. In the *second-stage*, a model predictive control algorithm has been proposed to compensate for the mismatch between profile realization of the PCC and determined dispatch plan of the *first-stage*.

In [5], it has been demonstrated that the optimal dispatch plan of distributed resources results in an infeasible or costly outcome when the ADN's hard security constraints are ignored. As a result, robust optimization in [5] has been written with ADN's hard security constraints. In [6], [7], the robust optimization method has been used to mitigate the ADN's congestion by reducing the variance of daily branch power flow while accounting for end-users' consumption and PV system production uncertainties. The dispatch plans have been set up in [8], [9] based on a *two-stage* adaptive robust optimization for calculating the optimal real/reactive power dispatch of PV systems within an ADN, which is robust against the uncertainties of PV system production capability. The importing and exporting of real power from the external network, as well as the energy transition of each BES system, have been determined in the *first-stage* of proposed problems. In the *second-stage*, cost of deviation from the *first-stage* plan, voltage magnitude deviations, and the cost of replanning BES

Manuscript received April 13, 2021; revised July 16, 2021, October 27, 2021, and January 11, 2022; accepted February 12, 2022. Date of publication February 25, 2022; date of current version June 21, 2022. This work was supported by the Swiss Federal Office of Energy through the ERA-NET Smart Energy Systems Regsys Joint Program 2019 in the frame of the project "DiGRiFlex-Real Time Distribution GRid control and Flexibility Provision Under Uncertainties." Paper no. TSG-00551-2021. *(Corresponding author: Mohammad Rayati.)*

Mohammad Rayati, Mokhtar Bozorg, and Mauro Carpita are with the Haute École d'Ingénierie et de Gestion du Canton de Vaud, Haute École Spécialisée de Suisse Occidentale, 1401 Yverdon-les-Bains, Switzerland (e-mail: mohammad.rayati@heig-vd.ch; mokhtar.bozorg@heig-vd.ch; mauro.carpita@heig-vd.ch).

Rachid Cherkaoui is with the Power System Research Group, École Polytechnique Fédérale de Lausanne, 1005 Lausanne, Switzerland (e-mail: rachid.cherkaoui@epfl.ch).

Color versions of one or more figures in this article are available at https://doi.org/10.1109/TSG.2022.3154023.

Digital Object Identifier 10.1109/TSG.2022.3154023

systems have been minimized considering the realized PV production capability. Distributionally robust chance constrained (DRCC) optimization problems have been developed to solve a real-time power dispatch problem in an ADN in [10], [11].

The provision of flexibility by distributed resources within the ADNs has been neglected in [2]–[11]. According to [12], the real/reactive power flexibility area of an ADN, including PV systems, has been determined using linear stochastic optimization. A framework for co-optimization of primary frequency control provision by a BES system has been proposed in [13]. A strategy for planning BES and PV systems to provide flexibility based on chance constrained (CC) optimization has been presented in [14]. An adaptive robust optimization for planning the dispatch of distributed resources, including PV and BES systems, has been developed in [15]. An adaptive robust restoration optimization involving the uncertainties of PV systems and end-users' consumption has been proposed in [16].

The gaps in previous studies for optimizing the dispatch plan of distributed resources in an ADN are fourfold:

- The hard security constraints of ADN, such as voltage and current constraints, have been ignored in studies such as [3], [4], [13], [14].
- The dispatch plan has been limited to determining the power profile at the PCC, not providing upward/downward real and reactive power flexibility. When flexibility has been included in the model, such as the models of [13], [14], it refers to droop-based real power control that is directly dependent on frequency deviation from the nominal value. Thus, historical frequency data are used as input, whereas statistical data about requests for flexibility by the external network's operator is not available if we want to consider both real/reactive power flexibility.
- The flexible resources have been bound to either the BES or PV systems. Compared to [8], [12], if we consider both kinds of distributed resources, then the problems of all time-steps must be solved in a single optimization problem, where managing the dimensions of the variables and constraints is a challenge.
- The proposed solution in [8]–[10] is a conservative dispatch plan for PV systems in ADNs, whereas a more optimal solution can be achieved such that the robustness against the uncertainties is not altered significantly.

B. Solution Approach

In this paper, we present a DRCC optimization problem to obtain the optimal dispatch plan of PV and BES systems within an ADN. The ADN's operator may apply the optimal dispatch plan for obtaining his bidding strategy in wholesale real/reactive power and flexibility markets. The difficulty for ADN's operators is that the probability density functions (PDFs) parameters of uncertainties are unknown. Because the data related to the uncertainties in ADNs are not available and obtaining an accurate prediction is not possible, the ambiguity set of PDFs is used.[1] Then, a DRCC optimization is developed to deal with the ambiguity set. In addition, we include the models and constraints of PV and BES systems in the decision-making process for obtaining the dispatch plan, as well as the ADN's hard security constraints.

In contrast to stochastic optimization, the DRCC optimization considers weaker assumptions on the exact PDFs of the uncertainties and utilizes a known portion of their statistical properties, such as moments of distribution or bounded deviation from a reference distribution. Compared with the robust optimization, the DRCC optimization reduces the conservativeness degree by exploiting data in the ambiguity set and demonstrates more statistically optimal performance.

The DRCC optimization problems have recently been studied in [18]–[21] to deal with ambiguity in the parameters of PDFs. Furthermore, the DRCC optimization problems have been used in a wide range of power system applications, including unit-commitment [22], [23], optimal power flow [24], [25], generation/transmission expansion planning [26], [27], ADN's optimization [10], [11], and so on.

Given the foregoing context, the paper's major contributions in terms of modeling and solution methodology are discussed in the following section.

C. Contributions

The following points are the contributions of this paper.

- An optimal dispatch plan for providing real/reactive power flexibility is presented based on DRCC optimization for the PV and BES systems within an ADN. The proposed optimal dispatch plan is robust against the uncertainties of PV systems' production capability, end-users' consumption, requested flexibility by the external network's operator, and the voltage magnitude at the PCC.
- The confidence level of satisfying chance constraints is introduced as an indicator of *flexibility quality*. Thus, the ADN's operator may provide low-*quality* to high-*quality* flexibility, with the ability to deviate from the flexibility requested by the external network's operator in real-time, providing the ADN's operator with an additional degree of freedom for optimal day-ahead planning.[2]
- From a modeling standpoint, in comparison to previous studies on DRCC optimization, we have to deal with several chance constraints and hard security constraints simultaneously. We present such a model because keeping the hard security constraints in an ADN is a must.
- For the proposed optimization problem, a solution methodology based on second-order conic programming[3] is presented.

D. Structure of the Paper

The mathematical formulation and the model of constraints for the described problem are presented in Section II. The DRCC optimization problem is formulated in Section III. A solution methodology is proposed in Section IV for solving

[1]For more information on ambiguity sets, see [17].

[2]The corresponding adjustable parameter for setting the confidence level in the proposed DRCC optimization, is explained in Section II-B.

[3]In a second-order conic program, a linear function is minimized over the intersection of an affine set and the product of second-order cones. The second-order conic programs are non-linear convex problems that include linear and convex quadratic programs [28].

the proposed DRCC optimization by a commercial or freely available solver. A numerical case study is given in V. Finally, Section VI concludes the paper. Appendix A presents the nomenclature. Additional seven appendices provide technical information that will be required throughout the paper.

II. Mathematical Formulation

A. Preliminary

The index for time is $t \in \mathcal{T}$, where $\mathcal{T} \coloneqq \{1, \ldots, T\}$. Buses other than the PCC are denoted by $n \in \mathcal{N}$, where $\mathcal{N} \coloneqq \{1, \ldots, N\}$. The PCC is represented by the index of 0. The PV and BES systems are indexed by i and s. The sets of PV and BES systems connected to bus n are denoted by $\mathcal{S}_n \coloneqq \{1, \ldots, S_n\}$ and $\mathcal{I}_n \coloneqq \{1, \ldots, I_n\}$, respectively.

We use lower-case and upper-case bold letters for the vectors and matrices, respectively. $(\cdot)^\top$ represents the transpose operator, $\mathbb{D}$ is a PDF, $\mathbb{E}^{\mathbb{D}}(\cdot)$ is the expectation operator over the PDF $\mathbb{D}$, $\mathbb{D}(\cdot)$ is the probability operator for the PDF $\mathbb{D}$.

There are no data available about the detailed PDF of uncertain parameters. However, the ambiguity set $\mathcal{D}$, i.e., the set of uncertainties' PDFs with predetermined first-order and second-order moments, as well as the lower-bound and upper-bound, is known. We consider the uncertain parameters with the magnitudes equal to the vector $\mathbf{m}+\boldsymbol{\zeta}$, where $\mathbf{m}$ is the mean forecast and $\boldsymbol{\zeta}$ is the forecast error with mean $\mathbf{0}$, covariance matrix Σ, minimum $\underline{\boldsymbol{\zeta}}$, and maximum $\bar{\boldsymbol{\zeta}}$. The ambiguity set $\mathcal{D}$ is defined as follows:

$$\mathcal{D} \coloneqq \left\{ \mathbb{D} \in \Psi^{(\mathcal{D})} : \mathbb{E}^{\mathbb{D}}(\boldsymbol{\zeta}) = \mathbf{0},\ \mathbb{E}^{\mathbb{D}}(\boldsymbol{\zeta} \cdot \boldsymbol{\zeta}^\top) = \Sigma, \underline{\boldsymbol{\zeta}} \le \boldsymbol{\zeta} \le \bar{\boldsymbol{\zeta}} \right\}, \tag{1}$$

where $\Psi(\mathcal{D})$ is the set of all possible PDFs. All $\mathbb{D}$ have first-order and second-order moments of $\mathbf{0}$ and Σ, respectively. The forecast error is also between $\underline{\boldsymbol{\zeta}}$ and $\bar{\boldsymbol{\zeta}}$.

The vectors of decision variables that are independent of uncertain parameters, the control variables of distributed resources, and the state variables are denoted by $\boldsymbol{z}$, $\boldsymbol{w}(\boldsymbol{\zeta})$, and $\boldsymbol{y}(\boldsymbol{\zeta})$, respectively.

There are two types of constraints in this paper: (i) the hard security constraints as defined in (2); (ii) the chance constraints as defined in (3).

$$\mathbb{D}\left[g_{hard}(\boldsymbol{z}, \boldsymbol{w}(\boldsymbol{\zeta}), \boldsymbol{y}(\boldsymbol{\zeta})) \le 0 \right] = 1, \quad \forall \mathbb{D} \in \mathcal{D}, \tag{2}$$

$$\inf_{\mathbb{D} \in \mathcal{D}} \mathbb{D}\left[g_{cc}(\boldsymbol{z}, \boldsymbol{w}(\boldsymbol{\zeta}), \boldsymbol{y}(\boldsymbol{\zeta})) \le 0 \right] \ge 1 - \epsilon, \tag{3}$$

where $1 - \epsilon \in [0, 1]$ is the chance constraint's confidence level. (2) denotes that the hard security constraints must be satisfied under uncertainties for each PDF instance in the ambiguity set (even the worst case of PDF instance)[4] On the other hand, (3) indicates that the probability of satisfying a constraint is greater than a confidence level under the uncertainties for the worst PDF in the ambiguity set.

It is worth mentioning that the ambiguity set in the context of this paper includes the moment information $\mathbf{0}$ and Σ, as well as support information $\underline{\boldsymbol{\zeta}}$ and $\bar{\boldsymbol{\zeta}}$, whereas the typical ambiguity sets only include the moment information [20]. In the context of this paper, the moment information is used for the chance constraints, while the support information is utilized in the hard security constraints to ensure that the ADN is completely secure considering the uncertainties. We could reformulate the proposed model of this paper such that the ambiguity set only contains moment information and all hard security constraints are also represented as chance constraints. The reformulated problem would then be equivalent to the model presented in this paper. However, we prefer the proposed model with simultaneous hard security and chance constraints for the following reasons: (i) The hard security constraints must be maintained with a confidence level close to one; and (ii) The ADN's operator can derive the support information $\underline{\boldsymbol{\zeta}}$ and $\bar{\boldsymbol{\zeta}}$ (the range of $\boldsymbol{\zeta}$) with a confidence level close to one and maintain the hard security constraints.

B. Modeling Objective Function of the ADN's Operator

In this section, we characterize the objective function of the ADN's operator. It should be noted that in this case, the ADN's operator does not reconfigure the network or change the transformer tap position to optimize the dispatch plan and flexibility because they are not changed on a daily basis. Furthermore, smart home participation and the binary variables associated with it are not taken into account.

Flexibility refers to the option of upward/downward movements of real/reactive power in real-time provided by the ADN for the use of the external network. The planned real/reactive power at the PCC are indicated as $p_t^{(PL)}$ and $q_t^{(PL)}$, respectively. The planned upward/downward real and reactive power flexibility are also denoted by $r_t^{(p\uparrow)}/r_t^{(p\downarrow)}$ and $r_t^{(q\uparrow)}/r_t^{(q\downarrow)}$. The planned flexibility is available for use according to the requirements of the external network's operator.

The objective of ADN's operator is to maximize his profit from selling real/reactive power, as well as the corresponding flexibility, as formulated in the following.

$$\max \ \text{objective} \coloneqq \boldsymbol{\lambda}^\top \cdot \boldsymbol{z}, \tag{5}$$

where the vector $\boldsymbol{z}$ is defined as the combination of planned real/reactive power and planned flexibility, i.e., $\boldsymbol{z} \coloneqq (p_t^{(PL)}, q_t^{(PL)}, r_t^{(p\uparrow)}, r_t^{(p\downarrow)}, r_t^{(q\uparrow)}, r_t^{(q\downarrow)})_{t\in\mathcal{T}}$; and the vector $\boldsymbol{\lambda}$ includes the prices of real/reactive power and flexibility.[5]

The external network's operator requests the planned capacity for real/reactive power flexibility in real-time. The requested real and reactive power flexibilities are denoted by $p_t^{(RE)}(\boldsymbol{\zeta})$ and $q_t^{(RE)}(\boldsymbol{\zeta})$, in which

$$r_t^{(p\downarrow)} \le p_t^{(RE)}(\boldsymbol{\zeta}) \le r_t^{(p\uparrow)}, \quad \forall t \in \mathcal{T}, \forall \boldsymbol{\zeta}, \tag{6}$$

$$-r_t^{(q\downarrow)} \le q_t^{(RE)}(\boldsymbol{\zeta}) \le r_t^{(q\uparrow)}, \quad \forall t \in \mathcal{T}, \forall \boldsymbol{\zeta}. \tag{7}$$

Because the behavior of the external network's operator when requesting the real/reactive power flexibility is dependent on many factors outside the framework of the ADN, the requested

[4]For ease of presentation, (2) is represented as (4) in the rest of the paper, which means that the hard security constraints must be satisfied for all instances of the forecast error vector..

$$g_{hard}(\boldsymbol{z}, \boldsymbol{w}(\boldsymbol{\zeta}), \boldsymbol{y}(\boldsymbol{\zeta})) \le 0, \ \forall \boldsymbol{\zeta}. \tag{4}$$

[5]It is worth mentioning that to find a bidding strategy to participate in the markets, the ADN's operator considers a set of values for the vector $\boldsymbol{\lambda}$. Then, the ADN's operator determines his bidding strategy based on the optimal value of $\boldsymbol{z}$ for each value of $\boldsymbol{\lambda}$.

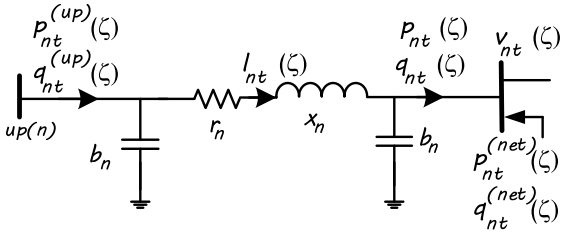

Fig. 1. Π-model of a distribution line.

real/reactive power is considered an ambiguous parameter, which is a function of $\boldsymbol{\zeta}$, where $p_t^{(RE)}(\boldsymbol{\zeta}) = \zeta_t^{(RE,p\downarrow)} \cdot r_t^{(p\downarrow)} + \zeta_t^{(RE,p\uparrow)} \cdot r_t^{(p\uparrow)}$ and $q_t^{(RE)}(\boldsymbol{\zeta}) = \zeta_t^{(RE,q\downarrow)} \cdot r_t^{(q\downarrow)} + \zeta_t^{(RE,q\uparrow)} \cdot r_t^{(q\uparrow)}$.

The following constraints must be embedded in the problem to tighten the feasible space and balance the ADN to provide flexibility in real-time. Therefore, it leads to several non-linear distributionally robust chance constraints (two-sided chance constraints), as shown below.

$$\inf_{\mathbb{D}\in\mathcal{D}} \mathbb{D}\Big[\Big|p_t^{(PL)} + p_t^{(RE)}(\boldsymbol{\zeta}) - p_{0t}(\boldsymbol{\zeta})\Big| \le \delta\Big] \ge 1-\epsilon, \quad \forall t \in \mathcal{T}, \tag{8}$$

$$\inf_{\mathbb{D}\in\mathcal{D}} \mathbb{D}\Big[\Big|q_t^{(PL)} + q_t^{(RE)}(\boldsymbol{\zeta}) - q_{0t}(\boldsymbol{\zeta})\Big| \le \delta\Big] \ge 1-\epsilon, \quad \forall t \in \mathcal{T}, \tag{9}$$

where $p_{0t}(\boldsymbol{\zeta})$ and $q_{0t}(\boldsymbol{\zeta})$ are real and reactive power available at the PCC for forecast error instance of $\boldsymbol{\zeta}$, respectively, and parameter δ is a small positive number, e.g., 0.01 kW, that refers to the maximum allowable deviation from the requested flexibility, i.e., $p_t^{(RE)}(\boldsymbol{\zeta})$ and $q_t^{(RE)}(\boldsymbol{\zeta})$, in addition to the dispatch plan at the PCC, i.e., $p_t^{(PL)}$ and $q_t^{(PL)}$. Because the ADN's power flow is a function of the uncertainties, $p_{0t}(\boldsymbol{\zeta})$ and $q_{0t}(\boldsymbol{\zeta})$ depends on $\boldsymbol{\zeta}$.[6]

For all PDFs in the ambiguity set $\mathcal{D}$ of the uncertain parameters, the actual real/reactive power provided by ADN's operator at the PCC differs from the requested flexibility by less than δ with minimum confidence level greater than $1-\epsilon$. By adjusting the parameter ϵ, the ADN's operator could provide low-*quality* to high-*quality* flexibility, giving him a degree of freedom, i.e., by loosening the obligation on him to provide the requested flexibility perfectly in real-time. As a result, the ADN's operator maximizes his objective function (5) while accounting for the chance constraints (8)-(9).

C. Power Flow Constraints

We consider a radial[7] ADN. The label "up(n)" denotes the bus that is upstream of the bus n, and the label "n" denotes the line whose downstream bus is the bus n. The binary parameter $u_{nn'}$ is defined, with $u_{nn'} = 1$ if $n' = \text{up}(n)$, otherwise $u_{nn'} = 0$. The Π-model of a distribution line is depicted in Fig. 1 for clarity and to introduce additional notations. Let $v_{nt}^{(up)}(\boldsymbol{\zeta})$ be the voltage square of bus "up(n)"; $p_{nt}^{(up)}(\boldsymbol{\zeta})$ and $q_{nt}^{(up)}(\boldsymbol{\zeta})$ represent the real and reactive power flows entering line n from bus "up(n)"; $p_{nt}(\boldsymbol{\zeta})$ and $q_{nt}(\boldsymbol{\zeta})$ denote the real and reactive power flow entering bus n from the bottom of line n, and $l_{nt}(\boldsymbol{\zeta})$ denotes the square of the current flowing in the central element of line n model. Finally, consider the resistance, reactance, and shunt impedance of line n to be r_n, x_n, and $2 \cdot b_n$, respectively.

Parameter $v_{0t}(\boldsymbol{\zeta})$ denotes the voltage square magnitude of the PCC at time t. Because the magnitude of the voltage at the PCC is affected by the external network's operation conditions, which include, among other factors, the voltage set-points at the power plants, and we lack the necessary data, $v_{0t}(\boldsymbol{\zeta}) = m_t^{(v)} + \zeta_t^{(v)}$ is regarded as an uncertain parameter and is written as a function of $\boldsymbol{\zeta}$. It is worth mentioning that we solve the problem for an ADN regardless of the neighboring distribution networks' dispatch plans.

The power flow constraints are presented in order to balance the injection and withdrawal of power on various buses. Let $p_{nt}^{(net)}(\boldsymbol{\zeta})$ and $q_{nt}^{(net)}(\boldsymbol{\zeta})$ represent the net real and reactive power injections to the bus n at time t, respectively.

$$p_{nt}^{(net)}(\boldsymbol{\zeta}) = \sum_{i\in\mathcal{I}_n} p_{it}^{(PV)}(\boldsymbol{\zeta}) + \sum_{s\in\mathcal{S}_n} p_{st}^{(BS)}(\boldsymbol{\zeta}) - p_{nt}^{(DM)}(\boldsymbol{\zeta}), \ \forall \boldsymbol{\zeta}, \tag{10}$$

$$q_{nt}^{(net)}(\boldsymbol{\zeta}) = \sum_{i\in\mathcal{I}_n} q_{it}^{(PV)}(\boldsymbol{\zeta}) + \sum_{s\in\mathcal{S}_n} q_{st}^{(BS)}(\boldsymbol{\zeta}) - q_{nt}^{(DM)}(\boldsymbol{\zeta}), \ \forall \boldsymbol{\zeta}, \tag{11}$$

where $p_{it}^{(PV)}(\boldsymbol{\zeta})$, $q_{it}^{(PV)}(\boldsymbol{\zeta})$, $p_{st}^{(BS)}(\boldsymbol{\zeta})$, and $q_{st}^{(BS)}(\boldsymbol{\zeta})$ are real power production of PV system i, reactive power of PV system i, real power output of BES system s, and reactive power output of BES system s, respectively. Here, the real and reactive power consumption of bus n are denoted by $p_{nt}^{(DM)}(\boldsymbol{\zeta})$ and $q_{nt}^{(DM)}(\boldsymbol{\zeta})$. Real and reactive power consumption are uncertain parameters and functions of $\boldsymbol{\zeta}$, i.e., $p_{nt}^{(DM)}(\boldsymbol{\zeta}) = m_{nt}^{(DM,p)} + \zeta_{nt}^{(DM,p)}$ and $q_{nt}^{(DM)}(\boldsymbol{\zeta}) = m_{nt}^{(DM,q)} + \zeta_{nt}^{(DM,q)}$.

For a given radial ADN, the power flow constraints are regarded as hard security constraints. They are defined as the intersection of several linear equalities and second-order conic inequalities for each instance of $\boldsymbol{\zeta}$.

$$\boldsymbol{\Omega}_{nt}^{(PF)}\Big(\boldsymbol{y}_{nt}^{(PF)}(\boldsymbol{\zeta})\Big) = 0, \quad \forall n \in \mathcal{N}, \forall t \in \mathcal{T}, \forall \boldsymbol{\zeta}, \tag{12}$$

$$\boldsymbol{\Gamma}_{nt}^{(PF)}\Big(\boldsymbol{y}_{nt}^{(PF)}(\boldsymbol{\zeta})\Big) \le 0, \quad \forall n \in \mathcal{N}, \forall t \in \mathcal{T}, \forall \boldsymbol{\zeta}, \tag{13}$$

where $\boldsymbol{\Omega}_{nt}^{(PF)}(\boldsymbol{y}_{nt}^{(PF)}(\boldsymbol{\zeta}))$ and $\boldsymbol{\Gamma}_{nt}^{(PF)}(\boldsymbol{y}_{nt}^{(PF)}(\boldsymbol{\zeta}))$ represent linear equalities and second-order conic inequalities of power flow, respectively, that are presented in detailed format in Appendix D; $\boldsymbol{y}_{nt}^{(PF)}(\boldsymbol{\zeta})$ is the state vector of the ADN that includes $p_{nt}^{(net)}(\boldsymbol{\zeta})$, $q_{nt}^{(net)}(\boldsymbol{\zeta})$, $p_{nt}^{(up)}(\boldsymbol{\zeta})$, $q_{nt}^{(up)}(\boldsymbol{\zeta})$, $p_{nt}(\boldsymbol{\zeta})$, $q_{nt}(\boldsymbol{\zeta})$, $v_{nt}^{(up)}(\boldsymbol{\zeta})$, $v_{nt}(\boldsymbol{\zeta})$, $l_{nt}(\boldsymbol{\zeta})$ and also the auxiliary variables as defined in Appendix D.

It is worth mentioning that the presented power flow constraints are exactly the ones introduced in [29]. As shown in [29], the introduced constraints give us the feasible space as AC exact power flow constraints for radial ADNs with reverse power flow.[8]

[6]With the same reasoning, all variables calculated by the power flow, as well as state/auxiliary variables of PV and BES systems, are written as functions of $\boldsymbol{\zeta}$ in the rest of the paper.

[7]This model can be applied to non-radial networks; however, the presented power flow model would be approximation.

[8]The necessary conditions for the exactness and convexity of the presented constraints have been given in [29, Th. I and Sec. IV]. For our case study in Section V of this paper, we confirm the validity of the necessary conditions.

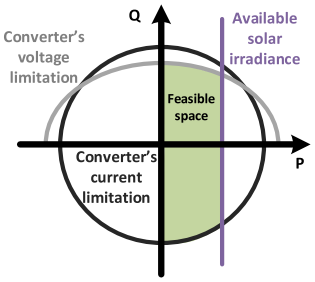

Fig. 2. Capability curve of a PV system [30].

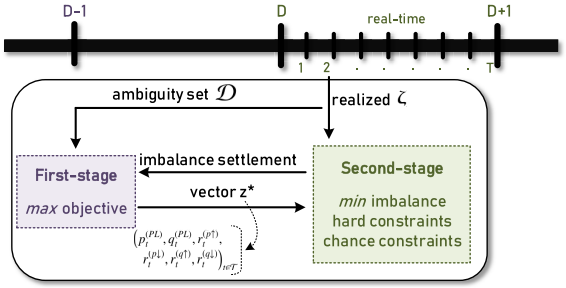

Fig. 3. Two-stage formulation of the ADN's optimization problem.

D. PV Systems' Capability Constraints

The capability curve of a PV system i is defined as the intersection of the following hard security constraints, illustrated in Fig. 2; (i) the voltage constraint of its converter, (ii) the current constraint of its converter, and (iii) the maximum allowable power production due to the solar irradiance.

The feasible space is modeled by several second-order conic inequalities for each instance of $\boldsymbol{\zeta}$, as shown below.

$$\boldsymbol{\Gamma}_{it}^{(PV)}\left(\boldsymbol{w}_{it}^{(PV)}(\boldsymbol{\zeta})\right) \leq 0, \quad \forall i \in \mathcal{I}_n, \forall n \in \mathcal{N}, \forall t \in \mathcal{T}, \forall \boldsymbol{\zeta}, \quad (14)$$

where $\boldsymbol{\Gamma}_{it}^{(PV)}(\boldsymbol{w}_{it}^{(PV)}(\boldsymbol{\zeta}))$ is the set of second-order conic inequalities of each PV system i that are presented in detailed format in Appendix C; $\boldsymbol{w}_{it}^{(PV)}(\boldsymbol{\zeta})$ is the control vector of PV system i at time t that is $(p_{it}^{(PV)}(\boldsymbol{\zeta}), q_{it}^{(PV)}(\boldsymbol{\zeta}))$.

Note that the solar irradiance is an uncertain parameter. The real power production of a PV system, i.e., $p_{it}^{(PV)}(\boldsymbol{\zeta})$, must be less than $p_{it}^{(PV,max)}(\boldsymbol{\zeta})$, which is an uncertain parameter and function of $\boldsymbol{\zeta}$, i.e., $p_{it}^{(PV,max)}(\boldsymbol{\zeta}) = m_{it}^{(PV,max)} + \zeta_{it}^{(PV,max)}$.

E. BES Systems Constraints

Each BES s is interfaced to the ADN by a converter. Therefore, the capability constraints of the converter must be governed in a hard manner. Furthermore, the energy balance known as the state-of-energy (SoE) of BES, which is denoted by $e_{st}(\boldsymbol{\zeta})$, must be taken into account.

The constraints are shown below in the form of a number of linear equalities and second-order conic inequalities for each instance of $\boldsymbol{\zeta}$.

$$\boldsymbol{\Omega}_{s}^{(BS)}\left(\boldsymbol{w}_{s}^{(BS)}(\boldsymbol{\zeta}), \boldsymbol{y}_{s}^{(BS)}(\boldsymbol{\zeta})\right) = 0, \quad \forall s \in \mathcal{S}_n, \forall n \in \mathcal{N}, \forall \boldsymbol{\zeta}, \quad (15)$$

$$\boldsymbol{\Gamma}_{s}^{(BS)}\left(\boldsymbol{w}_{s}^{(BS)}(\boldsymbol{\zeta}), \boldsymbol{y}_{s}^{(BS)}(\boldsymbol{\zeta})\right) \leq 0, \quad \forall s \in \mathcal{S}_n, \forall n \in \mathcal{N}, \forall \boldsymbol{\zeta}, \quad (16)$$

where $\boldsymbol{\Omega}_{s}^{(BS)}(\cdot)$ and $\boldsymbol{\Gamma}_{s}^{(BS)}(\cdot)$ are linear equalities and second-order conic inequalities of BES s, respectively, which are detailed in Appendix D; $\boldsymbol{w}_{s}^{(BS)}(\boldsymbol{\zeta})$ is the control vector of BES s that is $(p_{st}^{(BS)}(\boldsymbol{\zeta}), q_{st}^{(BS)}(\boldsymbol{\zeta}))_{t\in\mathcal{T}}$; and $\boldsymbol{y}_{s}^{(BS)}(\boldsymbol{\zeta})$ is the state vector that includes $(e_{st}(\boldsymbol{\zeta}))_{t\in\mathcal{T}}$ in addition to other auxiliary variables defined in Appendix D.

The considered constraints are based on the technique introduced in [31] for convexifying the constraints of BES systems. Instead of adding binary variables[9] to force a BES system to operate in one charging or discharging mode at each time-step, auxiliary continuous variables and convex constraints are added in this paper, as explained in Appendix D.

Here, the SoE at time 1, i.e., $e_{s1}(\boldsymbol{\zeta})$, is treated as an uncertain parameter. It is because the ADN's operator solves the optimization problem for obtaining the dispatch plan in advance, and the initial SoE of the BES systems is not determined until later in the day. As a result, the initial SoE of each BES s is expressed as a function of $\boldsymbol{\zeta}$, i.e., $e_{s1}(\boldsymbol{\zeta}) = m_{s}^{(BS)} + \zeta_{s}^{(BS)}$.

[9]See [32] for further information on using binary variables in the model of BES systems.

III. Optimal Dispatch Plan Based on DRCC

This section is dedicated to presenting the ADN operator's optimization problem for obtaining the optimal dispatch plan for PV and BES systems. Because it is assumed that the ADN's operator does not know the precise PDFs of uncertain parameters, the proposed optimization problem is based on DRCC and the resulting dispatch plan is distributionally robust.

The proposed optimization problem is expressed as *two-stage program with recourse* [33], as shown in Fig. 3. We have a set of decisions to make in a *two-stage program with recourse* that must be taken without full information about random events (i.e., uncertainties). These are known as *first-stage* decisions. Later, full information on the realization of random events is received. Following that, *second-stage* decisions or *recourse* actions are taken.

Here, the decision variables in the vector $\boldsymbol{z}$, which include the planned real/reactive power, as well as the planned flexibility, are determined in the *first-stage* by the ADN's operator. Then, the uncertain parameters in the vector $\boldsymbol{\zeta}$ are realized, and the ADN's operator takes his *recourse* actions to compensate for the uncertainties with available distributed resources in the *second-stage* and to meet the ADN's operating criteria, as well as the planned real/reactive power and requested flexibility.

The forecast error vector $\boldsymbol{\zeta}$ is as below.

$$\boldsymbol{\zeta} = \Bigg(\left(\zeta_{nt}^{(DM,p)}, \zeta_{nt}^{(DM,q)}, \left(\zeta_{it}^{(PV,max)}\right)_{i\in\mathcal{I}_n} \right)_{n\in\mathcal{N},t\in\mathcal{T}}, \left(\zeta_{s}^{(BS)}\right)_{s\in\mathcal{S}_n,n\in\mathcal{N}}, \left(\zeta_{t}^{(v)}, \zeta_{t}^{(RE,p\uparrow)}, \zeta_{t}^{(RE,p\downarrow)}\zeta_{t}^{(RE,q\uparrow)}, \zeta_{t}^{(RE,q\downarrow)}\right)_{t\in\mathcal{T}} \Bigg). \quad (17)$$

We want to incorporate the *second-stage* problem into the *first-stage* constraints. Then, there would be a single optimization problem that is solved in a one-shot. The available flexible resources for ADN's operator to compensate for the mismatch due to the uncertainties are variables in the vector $\boldsymbol{w}(\boldsymbol{\zeta}) = ((\boldsymbol{w}_{it}^{(PV)}(\boldsymbol{\zeta}))_{i\in\mathcal{I}_n}, (\boldsymbol{w}_{st}^{(BS)}(\boldsymbol{\zeta}))_{s\in\mathcal{S}_n})_{n\in\mathcal{N},t\in\mathcal{T}}$. To compensate for the mismatch, we employ a linear decision rule,[10] where the deviations in real/reactive power from forecast magnitudes are distributed linearly among the flexible resources. Thus, the control vector of distributed resources is

$$\boldsymbol{w}(\boldsymbol{\zeta}) = \hat{\mathbf{w}} + \boldsymbol{\alpha}\cdot\boldsymbol{\zeta}, \tag{18}$$

where,

$$\boldsymbol{\alpha}^{\top}\cdot\mathbf{1} = \mathbf{1}, \tag{19}$$

$$\mathbf{0} \preccurlyeq \boldsymbol{\alpha}. \tag{20}$$

Here, the vector $\hat{\mathbf{w}}$ represents the base point of PV and BES systems, the matrix $\boldsymbol{\alpha}$ represents distributed resources' participation factors for mitigation of uncertainties, $\mathbf{0}$ is a matrix with all elements equal to zero, and $\mathbf{1}$ is a vector with all elements equal to one. Note that (19) satisfies that the sum of each column of $\boldsymbol{\alpha}$ is equal to one, and by (20) each component of the matrix $\boldsymbol{\alpha}$ is greater than zero.[11]

To complete incorporating the *second-stage* problem into the *first-stage* constraints, we must determine the dependence of state vector $\boldsymbol{y}(\boldsymbol{\zeta}) = ((\boldsymbol{y}_{nt}^{(PF)}(\boldsymbol{\zeta}))_{n\in\mathcal{N},t\in\mathcal{T}}, (\boldsymbol{y}_{s}^{(BS)}(\boldsymbol{\zeta}))_{s\in\mathcal{S}_n,n\in\mathcal{N}}, (\boldsymbol{y}_{it}^{(PV)}(\boldsymbol{\zeta}))_{i\in\mathcal{I}_n,n\in\mathcal{N},t\in\mathcal{T}})$ on control vector $\boldsymbol{w}(\boldsymbol{\zeta})$ and forecast error vector $\boldsymbol{\zeta}$. To this end, we approximate the state vector $\boldsymbol{y}(\boldsymbol{\zeta})$ around $\hat{\mathbf{y}}$ as follows:

$$\boldsymbol{y}(\boldsymbol{\zeta}) = \hat{\mathbf{y}} + \boldsymbol{A}\cdot\boldsymbol{\zeta} - \boldsymbol{B}\cdot\boldsymbol{w}(\boldsymbol{\zeta}) = \left(\hat{\mathbf{y}} - \boldsymbol{B}\cdot\hat{\mathbf{w}}\right) + (\boldsymbol{A} - \boldsymbol{B}\cdot\boldsymbol{\alpha}).\boldsymbol{\zeta}, \tag{21}$$

where the matrices $\boldsymbol{A}$ and $\boldsymbol{B}$ include the sensitivity coefficients of the state variables to the uncertainties and control variables.

With a linear decision rule for the control vector (i.e., (18)-(20)) and the linearization of the state vector (i.e., (21)), we have the following one-shot DRCC optimization problem.

$$\max_{\Xi} \quad \text{objective} = (5) \tag{22}$$

$$\text{subject to:} \quad (8)-(16),\ (18)-(21), \tag{23}$$

where Ξ is the set of decision variables that is the union of the variables in the vectors $\hat{\mathbf{y}}$, $\hat{\mathbf{w}}$, $\boldsymbol{z}$, and the matrix $\boldsymbol{\alpha}$.

IV. Solution Methodology

The proposed DRCC optimization problem (22)-(23) cannot be solved directly by commercial solvers due to the non-linearity and infinite-dimensionality issues. The non-linearity is caused by the presence of the chance constraints (8)-(9). Furthermore, for all possible values of $\boldsymbol{\zeta}$, the constraints (10)-(16) must be satisfied, resulting in infinite-dimensionality. In this regard, we need an approximation solution such that the result would be viable for the original DRCC optimization problem (22)-(23).

In Section IV-A, we find a second-order conic approximation for the constraints (8)-(9). To overcome the issue of infinite dimensionality, we use the linear decision rule (18) to obtain a final model with a finite number of constraints that represent the worst-case of $\boldsymbol{\zeta}$ for (10)-(16) as described in Section IV-B. Eventually, the final optimization problem is a second-order conic program.

A. Approximating the Chance Constraints (8)-(9)

The chance constraints (8)-(9) are non-linear. We have not studied whether or not they represent convex space. We find the following second-order conic replacements for our chance constraints using a conservative approximation[12] as discussed in Appendix E.

$$\boldsymbol{a}_t^{(p)} = \left(\boldsymbol{R}_t^{(p)}\cdot\boldsymbol{z}\cdot\boldsymbol{M}_t^{(p)} - (\boldsymbol{h}_t^{(p)})^{\top}\cdot(\boldsymbol{A} - \boldsymbol{B}\cdot\boldsymbol{\alpha})\right)^{\top}, \quad \forall t\in\mathcal{T}, \tag{24}$$

$$\left(\boldsymbol{a}_t^{(p)}\right)^{\top}\cdot\Sigma\cdot\left(\boldsymbol{a}_t^{(p)}\right) + \gamma_t^{(p)} \le \epsilon\cdot\left(\delta - \theta_t^{(p)}\right), \quad \forall t\in\mathcal{T}, \tag{25}$$

$$\boldsymbol{a}_t^{(q)} = \left(\boldsymbol{R}_t^{(q)}\cdot\boldsymbol{z}\cdot\boldsymbol{M}_t^{(q)} - (\boldsymbol{h}_t^{(q)})^{\top}\cdot(\boldsymbol{A} - \boldsymbol{B}\cdot\boldsymbol{\alpha})\right)^{\top}, \quad \forall t\in\mathcal{T}, \tag{26}$$

$$\left(\boldsymbol{a}_t^{(q)}\right)^{\top}\cdot\Sigma\cdot\left(\boldsymbol{a}_t^{(q)}\right) + \gamma_t^{(q)} \le \epsilon\cdot\left(\delta - \theta_t^{(q)}\right), \quad \forall t\in\mathcal{T}, \tag{27}$$

$$\left|p_t^{(PL)} - (\boldsymbol{h}_t^{(p)})^{\top}\cdot(\hat{\mathbf{y}} - \boldsymbol{B}\cdot\hat{\mathbf{w}})\right| \le \gamma_t^{(p)} + \theta_t^{(p)}, \quad \forall t\in\mathcal{T}, \tag{28}$$

$$\left|q_t^{(PL)} - (\boldsymbol{h}_t^{(q)})^{\top}\cdot(\hat{\mathbf{y}} - \boldsymbol{B}\cdot\hat{\mathbf{w}})\right| \le \gamma_t^{(q)} + \theta_t^{(q)}, \quad \forall t\in\mathcal{T}, \tag{29}$$

$$0 \le \theta_t^{(p)} \le \delta, \quad \forall t\in\mathcal{T}, \tag{30}$$

$$0 \le \theta_t^{(q)} \le \delta, \quad \forall t\in\mathcal{T}, \tag{31}$$

$$0 \le \gamma_t^{(p)}, \quad \forall t\in\mathcal{T}, \tag{32}$$

$$0 \le \gamma_t^{(q)}, \quad \forall t\in\mathcal{T}, \tag{33}$$

where $\gamma_t^{(p)}$, $\gamma_t^{(q)}$, $\theta_t^{(p)}$, and $\theta_t^{(q)}$ are the auxiliary variables. Furthermore, the matrices $\boldsymbol{R}_t^{(p)}$, $\boldsymbol{R}_t^{(q)}$, $\boldsymbol{M}_t^{(p)}$, $\boldsymbol{M}_t^{(q)}$, and the vectors $\boldsymbol{h}_t^{(p)}$, $\boldsymbol{h}_t^{(q)}$ include the sensitivities of the chance constraints terms to the vector $\boldsymbol{z}$, $\boldsymbol{\zeta}$, and $\boldsymbol{y}(\boldsymbol{\zeta})$. The detailed definitions of $\boldsymbol{R}_t^{(p)}$, $\boldsymbol{R}_t^{(q)}$, $\boldsymbol{M}_t^{(p)}$, $\boldsymbol{M}_t^{(q)}$, $\boldsymbol{h}_t^{(p)}$, and $\boldsymbol{h}_t^{(q)}$ are given in Appendix E.

B. Relaxing the Hard Security Constraints (10)-(16)

The constraints (10)-(16) must be satisfied for all instances of $\boldsymbol{\zeta}$ in order to maintain the security of ADN and connected elements. The compact form of (10)-(16) is

$$\boldsymbol{\Gamma}(\boldsymbol{w}(\boldsymbol{\zeta}), \boldsymbol{y}(\boldsymbol{\zeta})) \le 0, \quad \forall\boldsymbol{\zeta}, \tag{34}$$

where $\boldsymbol{\Gamma}(\cdot)$ is defined as combination of $(\boldsymbol{\Omega}_s^{(BS)}(\cdot), -\boldsymbol{\Omega}_s^{(BS)}(\cdot), \boldsymbol{\Gamma}_s^{(BS)}(\cdot))_{s\in\mathcal{S}_n,n\in\mathcal{N}}$, $(\boldsymbol{\Gamma}_{it}^{(PV)}(\cdot))_{i\in\mathcal{I}_n,n\in\mathcal{N},t\in\mathcal{T}}$, and $(\boldsymbol{\Omega}_{nt}^{(PF)}(\cdot), -\boldsymbol{\Omega}_{nt}^{(PF)}(\cdot), \boldsymbol{\Gamma}_{nt}^{(PF)}(\cdot))_{n\in\mathcal{N},t\in\mathcal{T}}$.

To deal with the issue of infinite dimensionality, we rewrite the constraints (10)-(16) for the base-case and worst-case. As shown in the following (using (18) and (21)), we regard $\boldsymbol{\zeta}$ to be zero in the base-case.

$$\boldsymbol{\Gamma}\left(\hat{\mathbf{w}}, \hat{\mathbf{y}} - \boldsymbol{B}\cdot\hat{\mathbf{w}}\right) \le 0. \tag{35}$$

[10] Other non-linear decision rules have been described in [34], as well as their computational tractability.

[11] The component-wise less or equal operator for matrices is denoted by $\preccurlyeq$.

[12] Such conservative approximation is also explained in Appendix E.

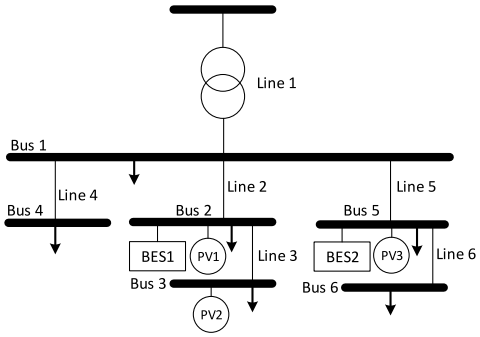

Fig. 4. Single-line diagram of the ADN for the case study.

For the worst-case, we include the following constraints in the optimization problem.

$$\max\left(\hat{\boldsymbol{y}} - \boldsymbol{B}\cdot\hat{\mathbf{w}} + (\boldsymbol{A} - \boldsymbol{B}\cdot\boldsymbol{\alpha})\cdot\boldsymbol{\zeta}\right) \leq \bar{\boldsymbol{y}}, \text{ subject to: } \underline{\boldsymbol{\zeta}} \leq \boldsymbol{\zeta} \leq \bar{\boldsymbol{\zeta}}, \tag{36}$$

$$\min\left(\hat{\boldsymbol{y}} - \boldsymbol{B}\cdot\hat{\mathbf{w}} + (\boldsymbol{A} - \boldsymbol{B}\cdot\boldsymbol{\alpha})\cdot\boldsymbol{\zeta}\right) \geq \underline{\boldsymbol{y}}, \text{ subject to: } \underline{\boldsymbol{\zeta}} \leq \boldsymbol{\zeta} \leq \bar{\boldsymbol{\zeta}}, \tag{37}$$

where $\bar{\boldsymbol{y}}$ and $\underline{\boldsymbol{y}}$ are maximum and minimum permissible range values for the state vector variables. It is worth mentioning that (36)-(37) is written component-wise because inequalities must be satisfied individually for each row of the vector.

The final optimization problem based on DRCC is

$$\max_{\Xi} \quad \text{objective} = (5) \tag{38}$$

$$\text{subject to:} \quad (19)-(20), (24)-(33), (35)-(37). \tag{39}$$

In the constraints of this final problem, there are several optimizations (36)-(37). Because we assume in (1) that we know the range of uncertainties, the optimizations (36)-(37) are over the range $[\underline{\boldsymbol{\zeta}}, \bar{\boldsymbol{\zeta}}]$. Furthermore, because the objectives of (36)-(37) are affine with respect to $\boldsymbol{\zeta}$, the value of $\underline{\boldsymbol{\zeta}}$ or $\bar{\boldsymbol{\zeta}}$ would be chosen based on the sign of each row of $(\boldsymbol{A} - \boldsymbol{B}\cdot\boldsymbol{\alpha})$. In Appendix F, the equivalent linear constraints to replace (36)-(37) are presented.

V. Numerical Case Study

A. Input Data

We use a case study based on a real low-voltage radial ADN in a rural area in Switzerland. Fig. 4 depicts the ADN in its abstract form. The ADN consists of three PV systems, two BES systems with capacities of 40 and 290 kWh, a transformer, and five distribution lines. Table I contains the data for ADN's parameters.

All simulations are run on an Intel Core i7-770 CPU with 3.6 GHz a clock speed and 32 GB of RAM. The source code is written in Python and Gurobi solver 9.1.

The inputs of the case study are PV power production and end-users' consumption on November 28^{th}, 2018. Furthermore, a forecasting method based on an autoregressive integrated moving average model is used. The sum of the mean forecast and error of real/reactive power of all buses is shown in Fig. 5.

TABLE I
Parameters of the ADN

Parameter	Value
Δt	10 min
$(r_n)_{n\in\mathcal{N}}$	$(0.0146, 0.263, 0.20, 0.096, 0.028, 0.018)$
$(x_n)_{n\in\mathcal{N}}$	$(0.0383, 0.078, 0.009, 0.072, 0.009, 0.005)$
$(2b_n)_{n\in\mathcal{N}}$	$(0.0000, 0.229, 0.0312, 0.241, 0.091, 0.015)$
$(S_i^{(PV,max)})_{i\in\mathcal{I}}$	(200 kW, 10 kW, 60 kW)
$(e_s^{(min)})_{s\in\mathcal{S}}$	$(0, 0)$
$(e_s^{(max)})_{s\in\mathcal{S}}$	(40 kWh,290 kWh)
$(\eta_s^{(C)})_{s\in\mathcal{S}}$	$(0.95, 0.95)$
$(\eta_s^{(D)})_{s\in\mathcal{S}}$	$(0.95, 0.95)$
δ	10^{-2} kW

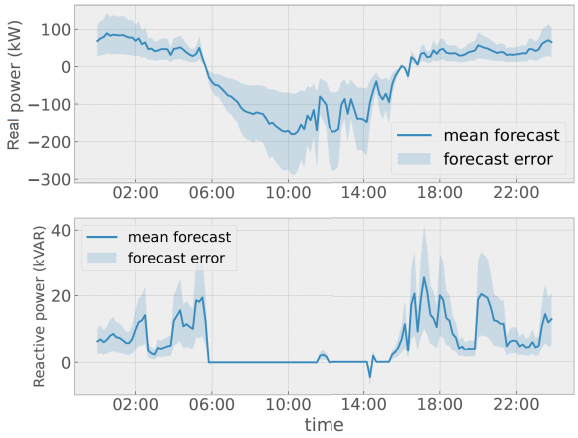

Fig. 5. The mean forecast and error of net real/reactive power.

B. Benchmark Optimization

We consider two benchmark models based on stochastic and CC optimization to evaluate the performance of the proposed DRCC dispatch plan. For stochastic optimization, historical data are used to generate a finite number of scenarios (i.e., instances of $\boldsymbol{\zeta}$) $\mathcal{K} = \{1, 2, \ldots, K\}$. Because the problem dimension is determined by the number of scenarios, i.e., K, we require a clustering approach for selecting the representative scenarios and ensuring a secure level of confidence with small K [35]. In Appendix H, we present the stochastic optimization problem for the ADN's dispatch plan.

For CC optimization, we have an assumption on the type of PDFs for the ambiguity set $\mathcal{D}$ in (1). We assume that the uncertain parameters have Gaussian PDF with a mean $\boldsymbol{m}$ and a covariance matrix $\boldsymbol{\Sigma}$. The optimization problem of ADN based on CC optimization is explained in Appendix G.

C. Results Comparison

The dispatch plans for various confidence levels are compared to the benchmark optimizations. For stochastic optimization, K is chosen to be equal to 100 and $1-\epsilon$ is chosen to be equal to 0.85 for CC optimization. The planned real/reactive power and flexibility for the benchmark optimizations and the proposed DRCC optimization with confidence levels of 0.75 and 0.90 are depicted in Figs. 6, 7, 8, and 9, respectively. By comparing the results, we arrive at the following conclusion:

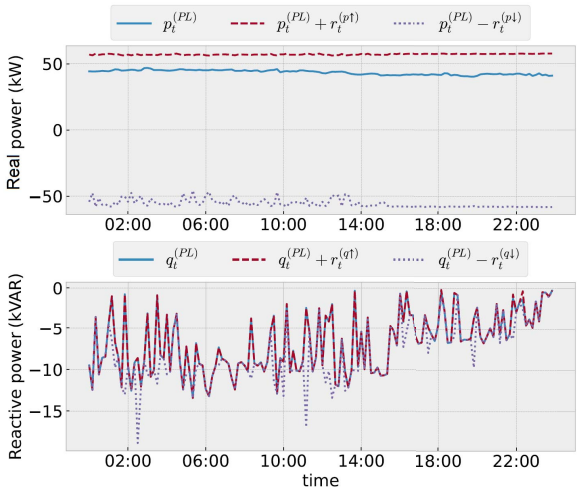

Fig. 6. Real/reactive power and flexibility for stochastic optimization.

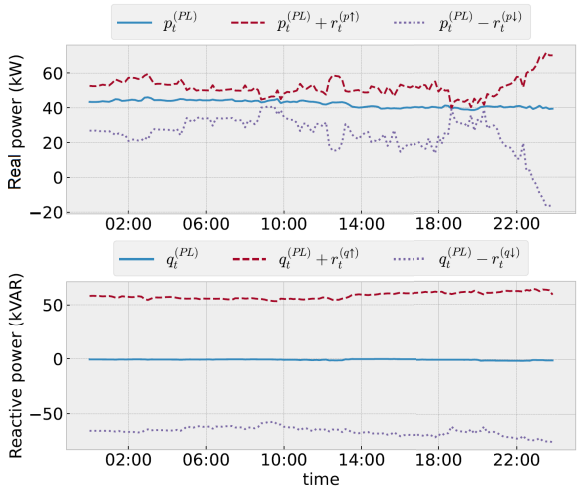

Fig. 7. Real/reactive power and flexibility for CC optimization with $1-\epsilon = 0.85$.

- Because of the nature of formulation, the result of DRCC is more conservative. We obtain a less conservative solution by lowering the confidence level, i.e., $1-\epsilon$.
- As distributed resources for upward real power flexibility are limited, increasing confidence level in the DRCC reduces upward real power flexibility significantly.
- More downward flexibility of real power is planned in the case of stochastic optimization compared to others.
- Despite the computational burden and increment of the required data, increasing the number of scenarios results in a more conservative dispatch plan.

In Fig. 10, the objective function of ADN's operator for different confidence levels and the benchmark models are compared. According to the results, the objective function does not decrease significantly with increasing confidence level. The objectives of stochastic and CC optimization, on the other hand, are higher at the expense of non-robustness against uncertainties and computational burden. Note that the dispatch plans based on stochastic and CC optimization are not robust against out-of-sample scenarios with varying PDFs.

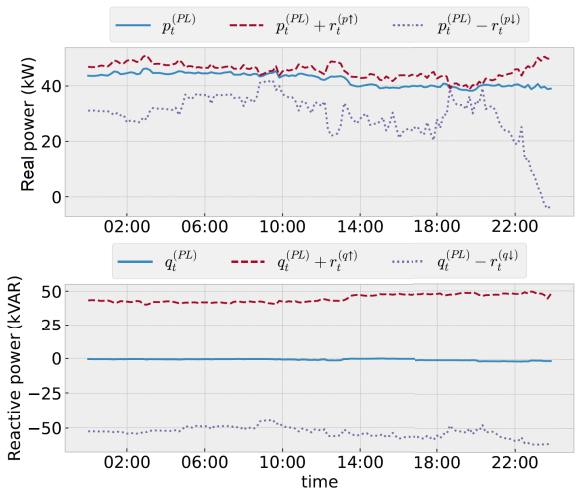

Fig. 8. Real/reactive power and flexibility for DRCC optimization with $1-\epsilon = 0.75$.

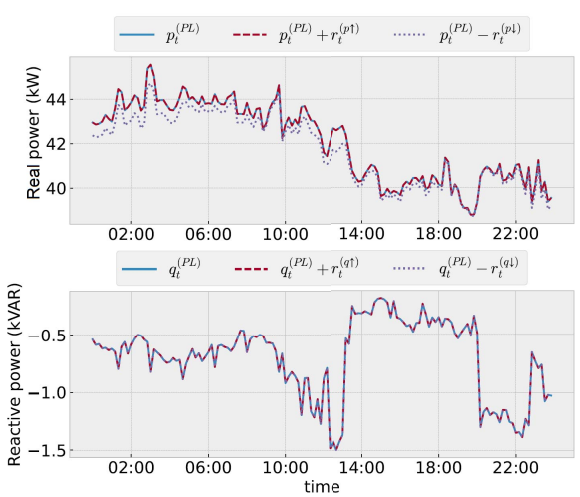

Fig. 9. Real/reactive power and flexibility for DRCC optimization with $1-\epsilon = 0.90$.

The computational time of DRCC for different confidence levels is between 2 to 3 minutes due to the decrement of the number of variables/constraints, whereas the solver needs more than 30 minutes to calculate the dispatch plan based on stochastic optimization when $K = 100$. The time required to solve the stochastic optimization grows exponentially with K, and the problem is unsolvable for large values of K.[13]

D. Out-of-Sample Analysis

Using Monte-Carlo simulation, we generate 200 out-of-sample scenarios (instances of $\boldsymbol{\zeta}$) for the stochastic, CC, and proposed DRCC formulations. We dispatch distributed resources for each time-step and for every out-of-sample scenario. The number of time-steps in a scenario where real/reactive power is deviated from the dispatch and requested flexibility by the external network's operator is then obtained. The deviation probability box diagram is shown in Fig. 11.

[13]In this case study, the stochastic optimization problem is unsolvable for $K > 300$.

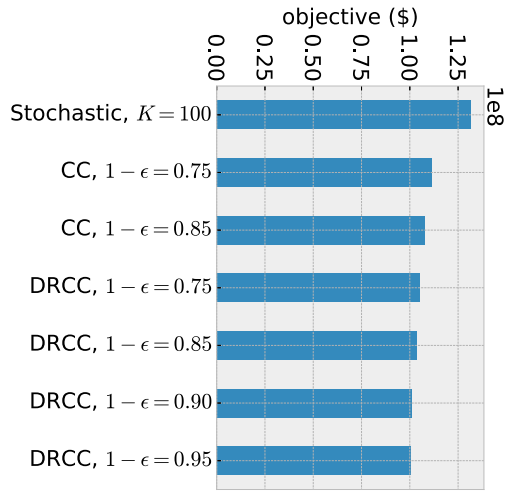

Fig. 10. Comparison of different optimizations in the objective.

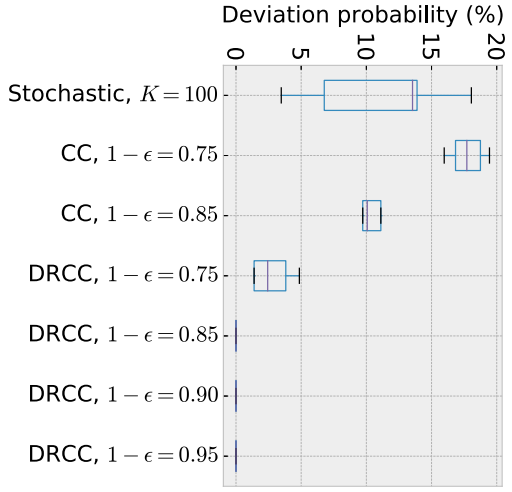

Fig. 11. Comparison of different optimizations in regards to the deviation probabilities in out-of-sample scenarios.

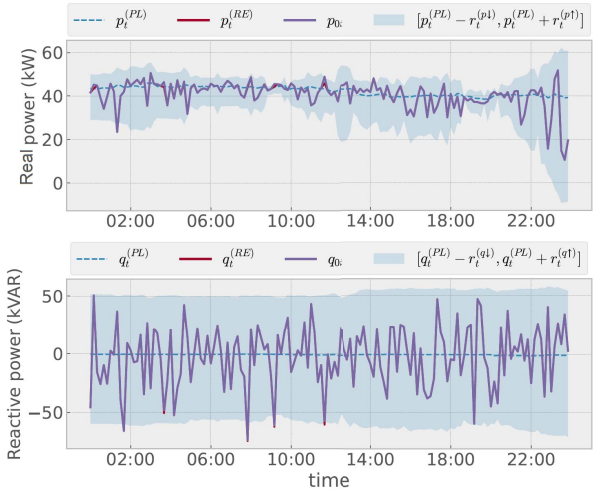

Fig. 12. Planned, requested, and actual real/reactive power and flexibility at the PCC of ADN with $1 - \epsilon = 0.90$.

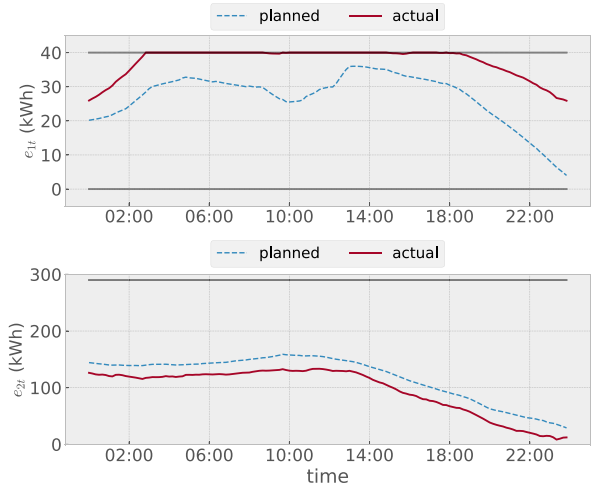

Fig. 13. Planned and actual SoE of BES systems.

As one can see, the stochastic and CC optimization problems have higher deviation probability. By increasing the confidence level, we obtain better *quality* in regards to the deviation probability at the cost of objective decrement.

E. Actual Operation

The DRCC dispatch plan with a confidence level of 0.90 is used to validate the proposed dispatch plan's performance in operation. The real data of the end-user's consumption and PV production on November 28^{th}, 2018 are used. Additionally, the flexibility request of the external network's operator is simulated. As shown in Fig. 12, the ADN's operator generally realizes the requested flexibility signal, with the exception of a few time-steps at 03:00 and 09:30.

The BES systems mitigate a large portion of the real/reactive power variations at the PCC. The SoE of two BES systems at buses 2 and 5 is shown in Fig. 13. The SoE of BES systems for the actual operation differs from the dispatch plan, but its feasibility has been preserved.

VI. Conclusion and Future Work

The resources within an ADN are dispatched to plan real/reactive power and flexibility while maintaining security and providing high-*quality* flexibility. To this end, a DRCC-based optimization problem is presented. The objective value of the ADN's operator is increased at the expense of less robustness against uncertainties by adjusting the confidence level of the chance constraints. As a result, the ADN's operator is free to defy the request of the external network's operator.

A case study compares the effectiveness of the proposed dispatch plan to the ones based on stochastic and CC optimization problems. When no data are available, the uncertain parameters can have any PDF. Furthermore, the computational complexity of the proposed formulation is significantly lower compared to the stochastic optimization. Finally, the obtained solution is more robust against the uncertainty.

In future work, smart home participation, transformers tap position change, and ADN's reconfiguration may be incorporated into the proposed optimization problem via binary

variables. Benders' decomposition algorithm can solve the resulting optimization problem. The proposed model implementation in a laboratory test environment is feasible. To this end, the environment of an adaptable ADN must be designed such that the PV and BES systems accept control signals from a central unit.

APPENDIX A
NOMENCLATURE

The main notations are defined in the following. Other symbols are defined as needed throughout the text.

Indices and Superscripts

n	Index of buses.
i	Index of PV systems.
s	Index of BES systems.
t	Index of time-steps.
k	Index of scenarios.
$\text{up}(n)$	Upstream bus of bus n.
PF	Power flow.
PV	Photovoltaic system.
BES	Battery energy storage system.
DM	End-users' consumption.
PL	Planned value.
RE	Requested magnitude.
net	Net power.
$\uparrow, \downarrow$	Upward and downward flexibility.
C	Charging.
D	Discharging.

Sets

$\mathcal{N}$	Set of buses.
$\mathcal{T}$	Set of time-steps.
$\mathcal{K}$	Set of scenarios.
$\mathcal{I}_n$	Set of PV systems of bus n.
$\mathcal{S}_n$	Set of BES systems of bus n.
$\mathcal{D}$	Ambiguity set.

Variables

v_{nt}	Voltage square of bus n.
l_{nt}	Square of the current flowing in the central eleme-nt of line n's model.
p_{nt}	Real power flow entering bus n from the bottom.
q_{nt}	Reactive power flow entering bus n from the bott-om.
$v_{nt}^{(up)}$	Voltage square of bus "up(n)".
$p_{nt}^{(up)}$	Real power flow entering bus n from the top.
$q_{nt}^{(up)}$	Reactive power flow entering bus n from the top.
$p_{nt}^{(DM)}$	Real power consumption of bus n.
$q_{nt}^{(DM)}$	Reactive power consumption of bus n.
$p_{it}^{(PV)}$	Real power production of PV system i.
$q_{it}^{(PV)}$	Reactive power production of PV system i.
$p_{st}^{(BS)}$	Real power production of BES system s.
$q_{st}^{(BS)}$	Reactive power production of BES system s.
$p_{nt}^{(net)}$	Net real power injection to bus n.
$q_{nt}^{(net)}$	Net reactive power injection to bus n.
e_{st}	SoE of BES system s.
$p_t^{(PL)}$	Planned real power at the PCC.
$q_t^{(PL)}$	Planned reactive power at the PCC.
$r_t^{(p\uparrow)}$	Planned upward real power flexibility.
$r_t^{(p\downarrow)}$	Planned downward real power flexibility.
$r_t^{(q\uparrow)}$	Planned upward reactive power flexibility.
$r_t^{(q\downarrow)}$	Planned downward reactive power flexibility.
$p_t^{(RE)}$	Requested real power in real-time.
$q_t^{(RE)}$	Requested reactive power in real-time.

Parameters

N	Numbers of buses.
I_n	Numbers of PV systems of bus n.
S_s	Numbers of BES systems of bus n.
T	Numbers of time-steps.
K	Numbers of scenarios.
Z	Numbers of uncertain parameters.
$u_{nn'}$	A binary parameter $u_{nn'}$, in which $u_{nn'} = 1$ if $n' = \text{up}(n)$ and $u_{nn'} = 0$ otherwise.
r_n	Resistance of line n.
x_n	Reactance of line n.
$2 \cdot b_n$	Shunt impedance of line n.
$1 - \epsilon$	Confidence level.
δ	Maximum allowable deviation from the requested real/reactive power.
$\eta_s^{(C)}$	Charging efficiency of BES system s.
$\eta_s^{(D)}$	Discharging efficiency of BES system s.
Δt	Time-step duration.

Vectors and Matrices

$\boldsymbol{m}$	Mean forecast vector.
$\boldsymbol{\zeta}$	Forecast error vector.
$\boldsymbol{\Sigma}$	Covariance matrix of forecast error vector.
$\boldsymbol{z}$	Vector of variables independent of uncertainties.
$\boldsymbol{w}(\boldsymbol{\zeta})$	Control vector of distributed resources.
$\boldsymbol{y}(\boldsymbol{\zeta})$	State vector of distributed resources and ADN.
$\bar{\boldsymbol{y}}, \underline{\boldsymbol{y}}$	Maximum and minimum range of the state vector.
$\boldsymbol{\lambda}$	Price vector.
$\bar{\boldsymbol{\zeta}}, \underline{\boldsymbol{\zeta}}$	Upper-bound and lower-bound of forecast error vector.
$\boldsymbol{\Omega}_{nt}^{(PF)}$	Equality constraints of power flow.
$\boldsymbol{\Gamma}_{nt}^{(PF)}$	Inequality constraints of power flow.
$\boldsymbol{y}_{nt}^{(PF)}$	State vector of the ADN.
$\boldsymbol{\Omega}_s^{(BS)}$	Equality constraints of BES system s.
$\boldsymbol{\Gamma}_s^{(BS)}$	Inequality constraints of BES system s.
$\boldsymbol{w}_s^{(BS)}$	Control vector of BES system s.
$\boldsymbol{y}_s^{(BS)}$	State variables vector of BES system s.
$\boldsymbol{\Gamma}_{it}^{(PV)}$	Inequality constraints of PV system i.
$\boldsymbol{w}_{it}^{(PV)}$	Control vector of PV system i.

APPENDIX B
DETAILS OF POWER FLOW CONSTRAINTS

For all buses $n \in \mathcal{N}$ and time-steps $t \in \mathcal{T}$ of a given radial ADN, the detailed power flow constraints $\boldsymbol{\Omega}_{nt}^{(PF)}(\boldsymbol{y}_{nt}^{(PF)}(\boldsymbol{\zeta}))$ and hard security constraints $\boldsymbol{\Gamma}_{nt}^{(PF)}(\boldsymbol{y}_{nt}^{(PF)}(\boldsymbol{\zeta}))$ are presented in the

following. It is worth mentioning that all variables must be functions of $\boldsymbol{\zeta}$ and all constraints must be satisfied for all instances of $\boldsymbol{\zeta}$ that are dropped here for the sake of brevity.

$$p_{nt}^{(up)} = r_n \cdot l_{nt} - p_{nt}^{(net)} + \sum_{n' \in \mathcal{N}} u_{nn'} \cdot p_{n't}^{(up)}, \tag{40}$$

$$q_{nt}^{(up)} = x_n \cdot l_{nt} - q_{nt}^{(net)} + \sum_{n' \in \mathcal{N}} u_{nn'} \cdot q_{n't}^{(up)} - \left(v_{nt} + v_{nt}^{(up)}\right) \cdot b_n, \tag{41}$$

$$v_{nt}^{(up)} = v_{nt} + 2\left(r_n \cdot p_{nt}^{(up)} + x_n \cdot (q_{nt}^{(up)} + v_{nt}^{(up)} \cdot b_n)\right) - \left(r_n^2 + x_n^2\right) \cdot l_{nt}, \tag{42}$$

$$l_{nt} \cdot v_{nt}^{(up)} \geq \left(p_{nt}^{(up)}\right)^2 + \left(q_{nt}^{(up)}\right)^2, \tag{43}$$

$$\hat{p}_{nt}^{(up)} = -p_{nt}^{(net)} + \sum_{n' \in \mathcal{N}} u_{nn'} \cdot \hat{p}_{n't}^{(up)}, \tag{44}$$

$$\hat{q}_{nt}^{(up)} = -q_{nt}^{(net)} + \sum_{n' \in \mathcal{N}} u_{nn'} \cdot \hat{q}_{n't}^{(up)} - \left(\bar{v}_{nt}^{(up)} + \bar{v}_{nt}\right) \cdot b_n, \tag{45}$$

$$\bar{v}_{nt}^{(up)} = \bar{v}_{nt} + 2\left(r_n \cdot \hat{p}_{nt}^{(up)} + x_n \cdot (\hat{q}_{nt}^{(up)} + \bar{v}_{nt}^{(up)} \cdot b_n)\right), \tag{46}$$

$$\bar{p}_{nt}^{(up)} = r_n \cdot \bar{l}_{nt} - p_{nt}^{(net)} + \sum_{n' \in \mathcal{N}} u_{nn'} \cdot \bar{p}_{n't}^{(up)}, \tag{47}$$

$$\bar{q}_{nt}^{(up)} = x_n \cdot \bar{l}_{nt} - q_{nt}^{(net)} + \sum_{n' \in \mathcal{N}} u_{nn'} \cdot \bar{q}_{n't}^{(up)} - \left(v_{nt} + v_{nt}^{(up)}\right) \cdot b_n, \tag{48}$$

$$\bar{l}_{nt} \cdot v_{nt} \geq \max\left\{\hat{p}_{nt}^2, \bar{p}_{nt}^2\right\} + \max\left\{(\hat{q}_{nt} - \bar{v}_{nt} \cdot b_n)^2 (\bar{q}_{nt} - v_{nt} \cdot b_n)^2\right\}, \tag{49}$$

$$\bar{l}_{nt} \cdot v_{nt}^{(up)} \geq \max\left\{(\hat{p}_{nt}^{(up)})^2, (\bar{p}_{nt}^{(up)})^2\right\} + \max\left\{(\hat{q}_{nt}^{(up)} + \bar{v}_{nt}^{(up)} \cdot b_n)^2, (\bar{q}_{nt}^{(up)} + v_{nt}^{(up)} \cdot b_n)^2\right\}, \tag{50}$$

$$\bar{p}_{nt} = -p_{nt}^{(net)} + \sum_{n' \in \mathcal{N}} u_{nn'} \cdot \bar{p}_{n't}^{(up)}, \tag{51}$$

$$\bar{q}_{nt} = -q_{nt}^{(net)} + \sum_{n' \in \mathcal{N}} u_{nn'} \cdot \bar{q}_{n't}^{(up)}, \tag{52}$$

$$\hat{p}_{nt} = -p_{nt}^{(net)} + \sum_{n' \in \mathcal{N}} u_{nn'} \cdot \hat{p}_{n't}^{(up)}, \tag{53}$$

$$\hat{q}_{nt} = -q_{nt}^{(net)} + \sum_{n' \in \mathcal{N}} u_{nn'} \cdot \hat{q}_{n't}^{(up)}, \tag{54}$$

$$l_n^{(max)} \cdot v_{nt} \geq \max\left\{\hat{p}_{nt}, \bar{p}_{nt}\right\}^2 + \max\left\{\hat{q}_{nt}, \bar{q}_{nt}\right\}^2, \tag{55}$$

$$l_n^{(max)} \cdot v_{nt}^{(up)} \geq \max\left\{\hat{p}_{nt}^{(up)}, \bar{p}_{nt}^{(up)}\right\}^2 + \max\left\{\hat{q}_{nt}^{(up)}, \bar{q}_{nt}^{(up)}\right\}^2, \tag{56}$$

$$v_n^{(min)} \leq |v_{nt}| \leq v_n^{(max)}, \tag{57}$$

where parameter $l_n^{(max)}$ is the maximum permissible value of current square for line n; parameters $v_n^{(min)}$ and $v_n^{(max)}$ are the minimum and maximum permissible magnitudes of voltage square of bus n. Here, the state vector $\boldsymbol{y}_{nt}^{(PF)}(\boldsymbol{\zeta})$ also includes the auxiliary variables $\hat{p}_{nt}^{(up)}(\boldsymbol{\zeta})$, $\hat{q}_{nt}^{(up)}(\boldsymbol{\zeta})$, $\bar{p}_{nt}^{(up)}(\boldsymbol{\zeta})$, $\bar{q}_{nt}^{(up)}(\boldsymbol{\zeta})$, $\hat{p}_{nt}(\boldsymbol{\zeta})$, $\hat{q}_{nt}(\boldsymbol{\zeta})$, $\bar{p}_{nt}(\boldsymbol{\zeta})$, $\bar{q}_{nt}(\boldsymbol{\zeta})$, $\bar{v}_{nt}(\boldsymbol{\zeta})$, $\bar{v}_{nt}^{(up)}(\boldsymbol{\zeta})$, and $\bar{l}_{nt}(\boldsymbol{\zeta})$;

APPENDIX C
DETAILS OF PV SYSTEMS' CONSTRAINTS

In the following, the detailed inequality constraints $\boldsymbol{\Gamma}_{it}^{(PV)}(\boldsymbol{w}_{it}^{(PV)}(\boldsymbol{\zeta}))$ of a PV system $i \in \mathcal{I}_n$ at time-step $t \in \mathcal{T}$ are given. As proven in [30], the converter's voltage constraint of a PV system is shown with a circle at the center of $-3(v_i^{(net,PV)})^2/x_i^{(PV)}$ in the Q-axis and a radius of $3v_i^{(net,PV)}v_i^{(con,PV)}/x_i^{(PV)}$.

$$\left(p_{it}^{(PV)}\right)^2 + \left(q_{it}^{(PV)} + \frac{3 \cdot (v_i^{(net,PV)})^2}{x_i^{(PV)}}\right)^2 \leq \left(\frac{3 \cdot v_i^{(net,PV)} \cdot v_i^{(con,PV)}}{x_i^{(PV)}}\right)^2, \tag{58}$$

where $v_i^{(net,PV)}$, $v_i^{(con,PV)}$, and $x_i^{(PV)}$ are the ADN's voltage, converter's voltage, and Thevenin reactance from the viewpoint of the PV system, respectively.

The converter's current constraint of a PV system $i \in \mathcal{I}_n$ at time-step $t \in \mathcal{T}$ is a circle with the radius of $S_i^{(PV,max)}$ as,

$$\left(p_{it}^{(PV)}\right)^2 + \left(q_{it}^{(PV)}\right)^2 \leq \left(S_i^{(PV,max)}\right)^2. \tag{59}$$

Finally, the constraint due to the available solar irradiance and the positive generation constraint of a PV system $i \in \mathcal{I}_n$ at time-step $t \in \mathcal{T}$ is also considered.

$$0 \leq p_{it}^{(PV)} \leq p_{it}^{(PV,max)}. \tag{60}$$

Note that all variables in (58)-(60) must be functions of $\boldsymbol{\zeta}$ and (58)-(60) must be satisfied for all instances of $\boldsymbol{\zeta}$ that are dropped here for the sake of brevity.

APPENDIX D
DETAILS OF BES SYSTEMS' CONSTRAINTS

For each BES $s \in \mathcal{S}_n$, the detailed equality constraints $\boldsymbol{\Omega}_s^{(BS)}(\boldsymbol{w}_s^{(BS)}(\boldsymbol{\zeta}), \boldsymbol{y}_s^{(BS)}(\boldsymbol{\zeta}))$ and inequality constraints $\boldsymbol{\Gamma}_s^{(BS)}(\boldsymbol{w}_s^{(BS)}(\boldsymbol{\zeta}), \boldsymbol{y}_s^{(BS)}(\boldsymbol{\zeta}))$ are presented in this section. It is worth mentioning that all variables must be functions of $\boldsymbol{\zeta}$ and all constraints must be satisfied for all instances of $\boldsymbol{\zeta}$ that are dropped here for the sake of brevity.

$$e_{s(t+1)} = e_{st} + \left(\frac{p_{st}^{(BS,D)}}{\eta_s^{(D)}} + \eta_s^{(C)} \cdot p_{st}^{(BS,C)}\right) \cdot \Delta t, \quad \forall t \in \mathcal{T} - \{T\}, \tag{61}$$

$$\leq p_{st}^{(BS,C)}, \quad \forall t \in \mathcal{T}, \tag{62}$$

$$0 \geq p_{st}^{(BS,D)}, \quad \forall t \in \mathcal{T}, \tag{63}$$

$$p_{st}^{(BS)} = p_{st}^{(BS,C)} + p_{st}^{(BS,D)}, \quad \forall t \in \mathcal{T}, \tag{64}$$

$$\left(p_{st}^{(BS)}\right)^2 + \left(q_{st}^{(BS)}\right)^2 \leq \left(S_s^{(BS,max)}\right)^2, \quad \forall t \in \mathcal{T}, \tag{65}$$

$$e_s^{(min)} \leq e_{st} \leq e_s^{(max)}, \quad \forall t \in \mathcal{T}, \tag{66}$$

$$\tilde{e}_{s(t+1)} = \tilde{e}_{st} + \left(p_{st}^{(BS,D)} + p_{st}^{(BS,C)}\right) \cdot \Delta t, \quad \forall t \in \mathcal{T} - \{T\}, \tag{67}$$

$$e_s^{(min)} \leq \tilde{e}_{st} \leq e_s^{(max)}, \quad \forall t \in \mathcal{T}, \tag{68}$$

where $\boldsymbol{y}_s^{(BS)}(\boldsymbol{\zeta}) = (p_{st}^{(BS,D)}(\boldsymbol{\zeta}), p_{st}^{(BS,C)}(\boldsymbol{\zeta}), \tilde{e}_{st}(\boldsymbol{\zeta}), e_{st}(\boldsymbol{\zeta}))_{t \in \mathcal{T}}$ is the vector of state variables; parameters $e_s^{(min)}$ and $e_s^{(max)}$

are the minimum and maximum permissible ranges of SoE; parameter $S_s^{(BS,max)}$ is the maximum apparent power flowing from the converter of BES system $s \in \mathcal{S}_n$.

Note that the constraints (67)-(68) and the auxiliary variable $\tilde{e}_{st}$ are added to the BES systems' model to prevent the usage of BES systems as unreal demand (e.g., charging and discharging at the same time) [31]. Thus, the proposed model is exact since it does not allow for simultaneous charging and discharging of the BES systems.

APPENDIX E
PROCESS OF APPROXIMATING THE CHANCE CONSTRAINTS

In this section, the process of approximation of (8)-(9) with second-order conic constraints (24)-(33) is explained. We start with (8)-(9) to find the functions $p_{0t}(\boldsymbol{\zeta})$ and $q_{0t}(\boldsymbol{\zeta})$ based on the linear decision rule (18) and linear approximation of state vector $\boldsymbol{y}(\boldsymbol{\zeta})$ around $\hat{\mathbf{y}}$ in (21). The functions $p_{0t}(\boldsymbol{\zeta})$ and $q_{0t}(\boldsymbol{\zeta})$ are elements of the state vector; thus, using vectors $\boldsymbol{h}_t^{(p)}$ and $\boldsymbol{h}_t^{(q)}$ are defined such that

$$p_{0t}(\boldsymbol{\zeta}) = (\boldsymbol{h}_t^{(p)})^\top \cdot \boldsymbol{y}(\boldsymbol{\zeta}), \tag{69}$$

$$q_{0t}(\boldsymbol{\zeta}) = (\boldsymbol{h}_t^{(q)})^\top \cdot \boldsymbol{y}(\boldsymbol{\zeta}). \tag{70}$$

By replacing (21) in (69)-(70), we have:

$$p_{0t}(\boldsymbol{\zeta}) = (\boldsymbol{h}_t^{(p)})^\top \cdot \left(\hat{\mathbf{y}} - \boldsymbol{B}\cdot\hat{\mathbf{w}}\right) + (\boldsymbol{h}_t^{(p)})^\top \cdot (\boldsymbol{A} - \boldsymbol{B}\cdot\boldsymbol{\alpha})\cdot\boldsymbol{\zeta}, \tag{71}$$

$$q_{0t}(\boldsymbol{\zeta}) = (\boldsymbol{h}_t^{(q)})^\top \cdot \left(\hat{\mathbf{y}} - \boldsymbol{B}\cdot\hat{\mathbf{w}}\right) + (\boldsymbol{h}_t^{(q)})^\top \cdot (\boldsymbol{A} - \boldsymbol{B}\cdot\boldsymbol{\alpha})\cdot\boldsymbol{\zeta}. \tag{72}$$

The functions $p_t^{(RE)}(\boldsymbol{\zeta})$ and $q_t^{(RE)}(\boldsymbol{\zeta})$ are reformulated as below by defining the matrices $\boldsymbol{R}_t^{(p)}$ and $\boldsymbol{R}_t^{(q)}$ properly.

$$\begin{aligned} p_t^{(RE)}(\boldsymbol{\zeta}) &= \zeta_t^{(RE,p\downarrow)}\cdot r_t^{(p\downarrow)} + \zeta_t^{(RE,p\uparrow)}\cdot r_t^{(p\uparrow)} \\ &= \boldsymbol{R}_t^{(p)}\cdot z\cdot \boldsymbol{M}_t^{(p)}\cdot\boldsymbol{\zeta}, \end{aligned} \tag{73}$$

$$\begin{aligned} q_t^{(RE)}(\boldsymbol{\zeta}) &= \zeta_t^{(RE,q\downarrow)}\cdot r_t^{(q\downarrow)} + \zeta_t^{(RE,q\uparrow)}\cdot r_t^{(q\uparrow)} \\ &= \boldsymbol{R}_t^{(q)}\cdot z\cdot \boldsymbol{M}_t^{(q)}\cdot\boldsymbol{\zeta}. \end{aligned} \tag{74}$$

By substituting $p_{0t}(\boldsymbol{\zeta})$, $q_{0t}(\boldsymbol{\zeta})$, $p_t^{(RE)}(\boldsymbol{\zeta})$, and $q_t^{(RE)}(\boldsymbol{\zeta})$ in (8)-(9) with (71)-(74), we obtain the following two-sided distributionally robust chance constraints.

$$\inf_{\mathbb{D}\in\mathcal{D}} \mathbb{D}\left[\left| b_t^{(p)}(\boldsymbol{x}) + \left(\boldsymbol{a}_t^{(p)}(\boldsymbol{x})\right)^\top\cdot\boldsymbol{\zeta}\right| \le \delta\right] \ge 1-\epsilon, \quad \forall t\in\mathcal{T}, \tag{75}$$

$$\inf_{\mathbb{D}\in\mathcal{D}} \mathbb{D}\left[\left| b_t^{(q)}(\boldsymbol{x}) + \left(\boldsymbol{a}_t^{(q)}(\boldsymbol{x})\right)^\top\cdot\boldsymbol{\zeta}\right| \le \delta\right] \ge 1-\epsilon, \quad \forall t\in\mathcal{T}, \tag{76}$$

where

$$\boldsymbol{a}_t^{(p)}(\boldsymbol{x}) = \left(\boldsymbol{R}_t^{(p)}\cdot z\cdot\boldsymbol{M}_t^{(p)} - \left(\boldsymbol{h}_t^{(p)}\right)^\top\cdot(\boldsymbol{A}-\boldsymbol{B}\cdot\boldsymbol{\alpha})\right)^\top, \tag{77}$$

$$b_t^{(p)}(\boldsymbol{x}) = p_t^{(PL)} - \left(\boldsymbol{h}_t^{(p)}\right)^\top\cdot\left(\hat{\mathbf{y}}-\boldsymbol{B}\cdot\hat{\mathbf{w}}\right), \tag{78}$$

$$\boldsymbol{a}_t^{(q)}(\boldsymbol{x}) = \left(\boldsymbol{R}_t^{(q)}\cdot z\cdot\boldsymbol{M}_t^{(q)} - \left(\boldsymbol{h}_t^{(q)}\right)^\top\cdot(\boldsymbol{A}-\boldsymbol{B}\cdot\boldsymbol{\alpha})\right)^\top, \tag{79}$$

$$b_t^{(q)}(\boldsymbol{x}) = q_t^{(PL)} - \left(\boldsymbol{h}_t^{(q)}\right)^\top\cdot\left(\hat{\mathbf{y}}-\boldsymbol{B}\cdot\hat{\mathbf{w}}\right), \tag{80}$$

and $\boldsymbol{x} = (\hat{\mathbf{y}}, \hat{\mathbf{w}}, z, \boldsymbol{\alpha})$.

Note that the ambiguity set $\mathcal{D}$ is a subset of the following set.

$$C \coloneqq \left\{\mathbb{D}\in\Psi^{(\mathcal{D})} : \mathbb{E}^{\mathbb{D}}(\boldsymbol{\zeta}) = \mathbf{0},\ \mathbb{E}^{\mathbb{D}}(\boldsymbol{\zeta}\cdot\boldsymbol{\zeta}^\top) = \Sigma\right\}, \tag{81}$$

Because $\mathcal{D}\subseteq C$, the left-hand-sides (LHSs) of (75)-(76) are greater than or equal to the LHSs of (82)-(83), respectively. Furthermore, the right-hand-sides (RHSs) of (75)-(76) are constant and equal to the RHSs of (82)-(83). Therefore, if we establish the following constraints, the original ones (75)-(76) also will be satisfied in a conservative manner. We approximate our original chance constraints with the following ones.

$$\inf_{\mathbb{D}\in C} \mathbb{D}\left[\left| b_t^{(p)}(\boldsymbol{x}) + \left(\boldsymbol{a}_t^{(p)}(\boldsymbol{x})\right)^\top\cdot\boldsymbol{\zeta}\right| \le \delta\right] \ge 1-\epsilon, \forall t\in\mathcal{T}, \tag{82}$$

$$\inf_{\mathbb{D}\in C} \mathbb{D}\left[\left| b_t^{(q)}(\boldsymbol{x}) + \left(\boldsymbol{a}_t^{(q)}(\boldsymbol{x})\right)^\top\cdot\boldsymbol{\zeta}\right| \le \delta\right] \ge 1-\epsilon, \forall t\in\mathcal{T}, \tag{83}$$

Each (82) and (83) is equivalent to the two-sided distributionally robust chance constraints introduced in equation (4) of [25]. Using [25, Th. II], the exact reformulation for (82) and (83) is as follows:

$$\gamma_t^{(p)} + \left(\boldsymbol{a}_t^{(p)}(\boldsymbol{x})\right)^\top\cdot\boldsymbol{\Sigma}\cdot\left(\boldsymbol{a}_t^{(p)}(\boldsymbol{x})\right) \le \epsilon\cdot\left(\delta-\theta_t^{(p)}\right), \quad \forall t\in\mathcal{T}, \tag{84}$$

$$\left| b_t^{(p)}(\boldsymbol{x})\right| \le \gamma_t^{(p)} + \theta_t^{(p)}, \quad \forall t\in\mathcal{T}, \tag{85}$$

$$0 \le \theta_t^{(p)} \le \delta, \quad \forall t\in\mathcal{T}, \tag{86}$$

$$0 \le \gamma_t^{(p)}, \quad \forall t\in\mathcal{T}, \tag{87}$$

$$\gamma_t^{(q)} + \left(\boldsymbol{a}_t^{(q)}(\boldsymbol{x})\right)^\top\cdot\boldsymbol{\Sigma}\cdot\left(\boldsymbol{a}_t^{(q)}(\boldsymbol{x})\right) \le \epsilon\cdot\left(\delta-\theta_t^{(q)}\right), \quad \forall t\in\mathcal{T}, \tag{88}$$

$$\left| b_t^{(q)}(\boldsymbol{x})\right| \le \gamma_t^{(q)} + \theta_t^{(q)}, \quad \forall t\in\mathcal{T}, \tag{89}$$

$$0 \le \theta_t^{(q)} \le \delta, \quad \forall t\in\mathcal{T}, \tag{90}$$

$$0 \le \gamma_t^{(q)}, \quad \forall t\in\mathcal{T}, \tag{91}$$

where $\gamma_t^{(p)}$, $\gamma_t^{(q)}$, $\theta_t^{(p)}$, and $\theta_t^{(q)}$ are the auxiliary variables. The resulting constraints (84)-(91) are equivalent to (24)-(33). Note that the feasible space given by the proposed reformulation is subset or equal to the feasible space given by (75) and (76).

APPENDIX F
LINEAR EQUIVALENTS OF WORST-CASE CONSTRAINTS

For each row m, the constraints (36)-(37) must be satisfied. The linear equivalent of row m of (36) is explained in this section. Other rows' constraints, as well as (37), can be rewritten using the same methodology.

We define the matrices $\boldsymbol{C}^{(pos)}$ and $\boldsymbol{C}^{(neg)}$ as follows:

$$\boldsymbol{C}^{(pos)} \coloneqq \mathrm{pos}(\boldsymbol{A}-\boldsymbol{\alpha}\cdot\boldsymbol{B}), \tag{92}$$

$$\boldsymbol{C}^{(neg)} \coloneqq \mathrm{neg}(\boldsymbol{A}-\boldsymbol{\alpha}\cdot\boldsymbol{B}), \tag{93}$$

where the function pos(·) gives 1 for each element of the input matrix if it is positive and otherwise 0, and the function neg(·) := 1 − pos(·).

Then, because the function inside maximizer (36) is affine with respect to $\boldsymbol{\zeta}$, the result of maximization for row m is as below.

$$\hat{y}_m - \boldsymbol{B}_m \cdot \hat{\mathbf{w}} + \boldsymbol{C}_m^{(pos)} \cdot \overline{\boldsymbol{\zeta}} - \boldsymbol{C}_m^{(neg)} \cdot \underline{\boldsymbol{\zeta}} \leq \overline{y}_m, \tag{94}$$

where $\boldsymbol{C}_m^{(pos)}$ and $\boldsymbol{C}_m^{(neg)}$ are the row m of the matrices $\boldsymbol{C}^{(pos)}$ and $\boldsymbol{C}^{(neg)}$, respectively.

It is worth mentioning that the sign of each element of $(\boldsymbol{A} - \boldsymbol{\alpha} \cdot \boldsymbol{B})$ appears to be influenced by the value of $\boldsymbol{\alpha}$. The signs are fixed for any value of $\boldsymbol{\alpha}$ due to (19)-(20) and the range of $\boldsymbol{A}$ and $\boldsymbol{B}$ for ADNs.

Appendix G
Chance Constraints With Gaussian PDF

By assuming Gaussian PDF for uncertainties, with a same method as [27, Appendix D], the chance constraints (75)-(76) are rewritten as follows:

$$b_t^{(p)}(\boldsymbol{x}) + \Phi^{-1}(1-\epsilon) \cdot \sqrt{\left(\boldsymbol{a}_t^{(p)}(\boldsymbol{x})\right)^\top \cdot \boldsymbol{\Sigma} \cdot \left(\boldsymbol{a}_t^{(p)}(\boldsymbol{x})\right)} \leq \delta, \forall t \in \mathcal{T}, \tag{95}$$

$$-b_t^{(p)}(\boldsymbol{x}) + \Phi^{-1}(1-\epsilon) \cdot \sqrt{\left(\boldsymbol{a}_t^{(p)}(\boldsymbol{x})\right)^\top \cdot \boldsymbol{\Sigma} \cdot \left(\boldsymbol{a}_t^{(p)}(\boldsymbol{x})\right)} \leq \delta, \forall t \in \mathcal{T}, \tag{96}$$

$$b_t^{(q)}(\boldsymbol{x}) + \Phi^{-1}(1-\epsilon) \cdot \sqrt{\left(\boldsymbol{a}_t^{(q)}(\boldsymbol{x})\right)^\top \cdot \boldsymbol{\Sigma} \cdot \left(\boldsymbol{a}_t^{(q)}(\boldsymbol{x})\right)} \leq \delta, \forall t \in \mathcal{T}, \tag{97}$$

$$-b_t^{(q)}(\boldsymbol{x}) + \Phi^{-1}(1-\epsilon) \cdot \sqrt{\left(\boldsymbol{a}_t^{(q)}(\boldsymbol{x})\right)^\top \cdot \boldsymbol{\Sigma} \cdot \left(\boldsymbol{a}_t^{(q)}(\boldsymbol{x})\right)} \leq \delta, \forall t \in \mathcal{T}, \tag{98}$$

where $\Phi^{-1}(1-\epsilon)$ is the inverse cumulative distribution of Gaussian PDF.

By replacing the constraints (24)-(31) in the problem (22) with (95)-(98), the final problem based on CC is as follows:

$$\max_{\Xi} \ \text{objective} = (5) \tag{99}$$

$$\text{subject to:} \quad (35)-(37),\ (95)-(98). \tag{100}$$

Appendix H
Dispatch Plan Based on Stochastic Optimization

For stochastic optimization, the original formulation is as follows:

$$\max_{\Xi_1} \ \text{objective} = (5) \tag{101}$$

$$\text{subject to:} \quad (8)-(16), \tag{102}$$

where Ξ_1 is the set of decision variables that is the union of the variables in the vectors $\boldsymbol{z}$, $\boldsymbol{w}(\boldsymbol{\zeta})$, and $\boldsymbol{y}(\boldsymbol{\zeta})$.

Here, a stochastic optimization based on second-order conic program is generated. Note that the DRCC formulation does not make any assumptions about the PDFs of the uncertain parameters. A randomized sampling approach, on the other hand, is required for stochastic optimization using historical data or an assumption of the PDFs of the uncertainties. Furthermore, the chance constraints in (8)-(9) are considered for all operation scenarios in stochastic optimization. Here, we assume Gaussian PDF for all uncertain parameters to generate the scenarios in stochastic optimization.

The chance constraints would be satisfied if the number of scenarios, i.e., K, is chosen large enough. The minimum number of scenarios for establishing different confidence levels is determined based on the results of [36].

By clustering the samples of historical data, we obtain a set of scenarios $\mathcal{K} = \{1, 2, \ldots, K\}$. Then, the optimization problem for obtaining the dispatch plan is as follows:

$$\max_{\Xi^{(ST)}} \ \text{objective} = (5) \tag{103}$$

subject to:

$$p_{ntk}^{(net)} = \sum_{i \in \mathcal{I}_n} p_{itk}^{(PV)} + \sum_{s \in \mathcal{S}_n} p_{stk}^{(BS)} - p_{ntk}^{(DM)}, \forall n, t, k, \tag{104}$$

$$q_{ntk}^{(net)} = \sum_{i \in \mathcal{I}_n} q_{itk}^{(PV)} + \sum_{s \in \mathcal{S}_n} q_{stk}^{(BS)} - q_{ntk}^{(DM)}, \forall n, t, k, \tag{105}$$

$$p_{ntk}^{(up)} = r_n \cdot l_{ntk} - p_{ntk}^{(net)} + \sum_{n' \in \mathcal{N}} u_{nn'} \cdot p_{n't}^{(up)}, \forall n, t, k, \tag{106}$$

$$q_{ntk}^{(up)} = x_n \cdot l_{ntk} - q_{ntk}^{(net)} + \sum_{n' \in \mathcal{N}} u_{nn'} \cdot q_{n't}^{(up)} - \left(v_{ntk} + v_{ntk}^{(up)}\right) \cdot b_n, \quad \forall n, t, k, \tag{107}$$

$$v_{ntk}^{(up)} = v_{ntk} + 2 \cdot \left(r_n \cdot p_{ntk}^{(up)} + x_n \cdot (q_{ntk}^{(up)} + v_{ntk}^{(up)} b_n)\right) - \left(r_n^2 + x_n^2\right) \cdot l_{ntk}, \forall n, t, k, \tag{108}$$

$$l_{ntk} v_{ntk}^{(up)} \geq \left(p_{ntk}^{(up)}\right)^2 + \left(q_{ntk}^{(up)}\right)^2, \forall n, t, k, \tag{109}$$

$$\hat{p}_{ntk}^{(up)} = -p_{ntk}^{(net)} + \sum_{n' \in \mathcal{N}} u_{nn'} \cdot \hat{p}_{n't}^{(up)}, \forall n, t, k, \tag{110}$$

$$\hat{q}_{ntk}^{(up)} = -q_{ntk}^{(net)} + \sum_{n' \in \mathcal{N}} u_{nn'} \cdot \hat{q}_{n't}^{(up)} - \left(\overline{v}_{ntk}^{(up)} + \overline{v}_{ntk}\right) \cdot b_n, \forall n, t, k, \tag{111}$$

$$\overline{v}_{ntk}^{(up)} = \overline{v}_{ntk} + 2 \cdot \left(r_n \cdot \hat{p}_{ntk}^{(up)} + x_n \cdot (\hat{q}_{ntk}^{(up)} + \overline{v}_{ntk}^{(up)} \cdot b_n)\right), \quad \forall n, t, k, \tag{112}$$

$$\overline{p}_{ntk}^{(up)} = r_n \cdot \bar{l}_{ntk} - p_{ntk}^{(net)} + \sum_{n' \in \mathcal{N}} u_{nn'} \cdot \overline{p}_{n't}^{(up)}, \forall n, t, k, \tag{113}$$

$$\overline{q}_{ntk}^{(up)} = x_n \cdot \bar{l}_{ntk} - q_{ntk}^{(net)} + \sum_{n' \in \mathcal{N}} u_{nn'} \cdot \overline{q}_{n't}^{(up)} - \left(v_{ntk} + v_{ntk}^{(up)}\right) \cdot b_n, \forall n, t, k, \tag{114}$$

$$\bar{l}_{ntk} v_{ntk} \geq \max\left\{\hat{p}_{ntk}^2, \overline{p}_{ntk}^2\right\} + \max\left\{(\hat{q}_{ntk} - \overline{v}_{ntk} \cdot b_n)^2, (\overline{q}_{ntk} - v_{ntk} \cdot b_n)^2\right\}, \forall n, t, k, \tag{115}$$

$$\bar{l}_{ntk} v_{ntk}^{(up)} \geq \max\left\{(\hat{p}_{ntk}^{(up)})^2, (\overline{p}_{ntk}^{(up)})^2\right\} + \max\left\{(\hat{q}_{ntk}^{(up)} + \overline{v}_{ntk}^{(up)} \cdot b_n)^2, (\overline{q}_{ntk}^{(up)} + v_{ntk}^{(up)} \cdot b_n)^2\right\}, \quad \forall n, t, k, \tag{116}$$

$$\overline{p}_{ntk} = -p^{(net)}_{ntk} + \sum_{n' \in \mathcal{N}} u_{nn'} \cdot \overline{p}^{(up)}_{n't}, \forall n, t, k, \tag{117}$$

$$\overline{q}_{ntk} = -q^{(net)}_{ntk} + \sum_{n' \in \mathcal{N}} u_{nn'} \cdot \overline{q}^{(up)}_{n't}, \forall n, t, k, \tag{118}$$

$$\hat{p}_{ntk} = -p^{(net)}_{ntk} + \sum_{n' \in \mathcal{N}} u_{nn'} \cdot \hat{p}^{(up)}_{n't}, \forall n, t, k, \tag{119}$$

$$\hat{q}_{ntk} = -q^{(net)}_{ntk} + \sum_{tn' \in \mathcal{N}} u_{nn'} \cdot \hat{q}^{(up)}_{n't}, \forall n, t, k, \tag{120}$$

$$l^{(max)}_n \cdot v_{ntk} \geq \max\left\{\hat{p}_{ntk}, \overline{p}_{ntk}\right\}^2 + \max\left\{\hat{q}_{ntk}, \overline{q}_{ntk}\right\}^2, \quad \forall n, t, k, \tag{121}$$

$$l^{(max)}_n \cdot v^{(up)}_{ntk} \geq \max\left\{\hat{p}^{(up)}_{ntk}, \overline{p}^{(up)}_{ntk}\right\}^2 + \max\left\{\hat{q}^{(up)}_{ntk}, \overline{q}^{(up)}_{ntk}\right\}^2, \quad \forall n, t, k, \tag{122}$$

$$v^{(min)}_n \leq |v_{ntk}| \leq v^{(max)}_n, \forall n, t, k, \tag{123}$$

$$e_{s(t+1)k} = e_{stk} + \left(\frac{p^{(BS,D)}_{stk}}{\eta^{(D)}_s} + \eta^{(C)}_s \cdot p^{(BS,C)}_{stk}\right) \cdot \Delta t, \forall s, t, k, \tag{124}$$

$$0 \leq p^{(BS,C)}_{stk}, \forall s, t, k, \tag{125}$$

$$0 \geq p^{(BS,D)}_{stk}, \forall s, t, k, \tag{126}$$

$$p^{(BS)}_{stk} = p^{(BS,C)}_{stk} + p^{(BS,D)}_{stk}, \forall s, t, k, \tag{127}$$

$$(p^{(BS)}_{stk})^2 + (q^{(BS)}_{stk})^2 \leq (S^{(BS,max)}_s)^2, \forall s, t, k, \tag{128}$$

$$e^{(min)}_s \leq e_{stk} \leq e^{(max)}_s, \forall s, t, k, \tag{129}$$

$$\tilde{e}_{s(t+1)k} = \tilde{e}_{stk} + \left(p^{(BS,D)}_{stk} + p^{(BS,C)}_{stk}\right) \cdot \Delta t, \forall s, t, k, \tag{130}$$

$$e^{(min)}_s \leq \tilde{e}_{stk} \leq e^{(max)}_s, \forall s, t, k, \tag{131}$$

$$\left(p^{(PV)}_{itk}\right)^2 + \left(q^{(PV)}_{itk} + \frac{3 \cdot (v^{(net,PV)}_i)^2}{x^{(PV)}_i}\right)^2 \leq \left(\frac{3 \cdot v^{(net,PV)}_i \cdot v^{(con,PV)}_i}{x^{(PV)}_i}\right)^2, \quad \forall i, t, k, \tag{132}$$

$$\left(p^{(PV)}_{itk}\right)^2 + \left(q^{(PV)}_{itk}\right)^2 \leq \left(S^{(PV,max)}_i\right)^2, \forall i, t, k, \tag{133}$$

$$0 \leq p^{(PV)}_{itk} \leq p^{(PV,max)}_{itk}, \forall i, t, k, \tag{134}$$

$$\left|p^{(PL)}_t + p^{(RE)}_{tk} - p_{0tk}\right| \leq \delta, \forall t, k, \tag{135}$$

$$\left|q^{(PL)}_t + q^{(RE)}_{tk} - q_{0tk}\right| \leq \delta, \forall t, k. \tag{136}$$

REFERENCES

[1] X. Jin, Q. Wu, and H. Jia, "Local flexibility markets: Literature review on concepts, models and clearing methods," *Appl. Energy*, vol. 261, Mar. 2020, Art. no. 114387.

[2] Y. Jin, Z. Wang, C. Jiang, and Y. Zhang, "Dispatch and bidding strategy of active distribution network in energy and ancillary services market," *J. Modern Power Syst. Clean Energy*, vol. 3, no. 4, pp. 565–572, 2015.

[3] G. Liu, Y. Xu, and K. Tomsovic, "Bidding strategy for microgrid in day-ahead market based on hybrid stochastic/robust optimization," *IEEE Trans. Smart Grid*, vol. 7, no. 1, pp. 227–237, Jan. 2016.

[4] F. Sossan, E. Namor, R. Cherkaoui, and M. Paolone, "Achieving the dispatchability of distribution feeders through prosumers data driven forecasting and model predictive control of electrochemical storage," *IEEE Trans. Sustain. Energy*, vol. 7, no. 4, pp. 1762–1777, Oct. 2016.

[5] A. Sadeghi-Mobarakeh, A. Shahsavari, H. Haghighat, and H. Mohsenian-Rad, "Optimal market participation of distributed load resources under distribution network operational limits and renewable generation uncertainties," *IEEE Trans. Smart Grid*, vol. 10, no. 4, pp. 3549–3561, Jul. 2019.

[6] X. Yan, C. Gu, X. Zhang, and F. Li, "Robust optimization-based energy storage operation for system congestion management," *IEEE Syst. J.*, vol. 14, no. 2, pp. 2694–2702, Jun. 2020.

[7] J. Zhao, Y. Wang, G. Song, P. Li, C. Wang, and J. Wu, "Congestion management method of low-voltage active distribution networks based on distribution locational marginal price," *IEEE Access*, vol. 7, pp. 32240–32255, 2019.

[8] T. Ding, C. Li, Y. Yang, J. Jiang, Z. Bie, and F. Blaabjerg, "A two-stage robust optimization for centralized-optimal dispatch of photovoltaic inverters in active distribution networks," *IEEE Trans. Sustain. Energy*, vol. 8, no. 2, pp. 744–754, Apr. 2017.

[9] M. Nick, M. Bozorg, R. Cherkaoui, and M. Paolone, "A robust optimization framework for the day-ahead scheduling of active distribution networks including energy storage systems," in *Proc. IEEE Milan PowerTech*, 2019, pp. 1–6.

[10] Y. Yang and W. Wu, "A distributionally robust optimization model for real-time power dispatch in distribution networks," *IEEE Trans. Smart Grid*, vol. 10, no. 4, pp. 3743–3752, Jul. 2019.

[11] A. Bagchi and Y. Xu, "Distributionally robust chance-constrained bidding strategy for distribution system aggregator in day-ahead markets," in *Proc. IEEE Int. Conf. Commun. Control Comput. Technol. Smart Grids*, 2018, pp. 1–6.

[12] M. Kalantar-Neyestanaki, F. Sossan, M. Bozorg, and R. Cherkaoui, "Characterizing the reserve provision capability area of active distribution networks: A linear robust optimization method," *IEEE Trans. Smart Grid*, vol. 11, no. 3, pp. 2464–2475, May 2020.

[13] J. Engels, B. Claessens, and G. Deconinck, "Combined stochastic optimization of frequency control and self-consumption with a battery," *IEEE Trans. Smart Grid*, vol. 10, no. 2, pp. 1971–1981, Mar. 2019.

[14] F. Conte, S. Massucco, G. P. Schiapparelli, and F. Silvestro, "Day-ahead and intra-day planning of integrated BESS-PV systems providing frequency regulation," *IEEE Trans. Sustain. Energy*, vol. 11, no. 3, pp. 1797–1806, Jul. 2020.

[15] K. Christakou, M. Paolone, and A. Abur, "Voltage control in active distribution networks under uncertainty in the system model: A robust optimization approach," *IEEE Trans. Smart Grid*, vol. 9, no. 6, pp. 5631–5642, Nov. 2018.

[16] X. Chen, W. Wu, and B. Zhang, "Robust Restoration method for active distribution networks," *IEEE Trans. Power Syst.*, vol. 31, no. 5, pp. 4005–4015, Sep. 2016.

[17] B. L. Gorissen, İ. Yanıkoğlu, and D. den Hertog, "A practical guide to robust optimization," *Omega*, vol. 53, pp. 124–137, Jun. 2015.

[18] X. Chen, M. Sim, and P. Sun, "A robust optimization perspective on stochastic programming," *Oper. Res.*, vol. 55, no. 6, pp. 1058–1071, 2007.

[19] I. Popescu, "Robust mean-covariance solutions for stochastic optimization," *Oper. Res.*, vol. 55, no. 1, pp. 98–112, 2007.

[20] D. Bertsimas, M. Sim, and M. Zhang, "Adaptive distributionally robust optimization," *Manag. Sci.*, vol. 65, no. 2, pp. 604–618, 2019.

[21] S. Zymler, D. Kuhn, and B. Rustem, "Distributionally robust joint chance constraints with second-order moment information," *Math. Program.*, vol. 137, no. 1, pp. 167–198, 2013.

[22] P. Xiong, P. Jirutitijaroen, and C. Singh, "A distributionally robust optimization model for unit commitment considering uncertain wind power generation," *IEEE Trans. Power Syst.*, vol. 32, no. 1, pp. 39–49, Jan. 2017.

[23] Y. Zhou, M. Shahidehpour, Z. Wei, Z. Li, G. Sun, and S. Chen, "Distributionally robust unit commitment in coordinated electricity and district heating networks," *IEEE Trans. Power Syst.*, vol. 35, no. 3, pp. 2155–2166, May 2020.

[24] Y. Zhang, S. Shen, and J. L. Mathieu, "Distributionally robust chance-constrained optimal power flow with uncertain renewables and uncertain reserves provided by loads," *IEEE Trans. Power Syst.*, vol. 32, no. 2, pp. 1378–1388, Mar. 2017.

[25] W. Xie and S. Ahmed, "Distributionally robust chance constrained optimal power flow with renewables: A conic reformulation," *IEEE Trans. Power Syst.*, vol. 33, no. 2, pp. 1860–1867, Mar. 2018.

[26] D. Alvarado, A. Moreira, R. Moreno, and G. Strbac, "Transmission network investment with distributed energy resources and distributionally robust security," *IEEE Trans. Power Syst.*, vol. 34, no. 6, pp. 5157–5168, Nov. 2019.

[27] F. Pourahmadi, J. Kazempour, C. Ordoudis, P. Pinson, and S. H. Hosseini, "Distributionally robust chance-constrained generation expansion planning," *IEEE Trans. Power Syst.*, vol. 35, no. 4, pp. 2888–2903, Jul. 2020.

[28] S. Huang, K. Filonenko, and C. T. Veje, "A review of the convexification methods for AC optimal power flow," in *Proc. IEEE Electr. Power Energy Conf. (EPEC)*, 2019, pp. 1–6.

[29] M. Nick, R. Cherkaoui, J.-Y. Le Boudec, and M. Paolone, "An exact convex formulation of the optimal power flow in radial distribution networks including transverse components," *IEEE Trans. Autom. Control*, vol. 63, no. 3, pp. 682–697, Mar. 2018.

[30] A. Cabrera-Tobar, E. Bullich-Massagué, M. Aragüés-Peñalba, and O. Gomis-Bellmunt, "Capability curve analysis of photovoltaic generation systems," *Solar Energy*, vol. 140, pp. 255–264, Dec. 2016.

[31] M. Nick, "Exact convex modeling of the optimal power flow for the operation and planning of active distribution networks with energy storage systems," Ph.D. dissertation, Doctorat Génie Électrique, École Polytechnique Fédérale de Lausanne, Lausanne, Switzerland, 2016.

[32] J. M. Arroyo, L. Baringo, A. Baringo, R. Bolaños, N. Alguacil, and N. G. Cobos, "On the use of a convex model for bulk storage in MIP-based power system operation and planning," *IEEE Trans. Power Syst.*, vol. 35, no. 6, pp. 4964–4967, Nov. 2020.

[33] J. R. Birge and F. Louveaux, *Introduction to Stochastic Programming*. New York, NY, USA: Springer, 2011.

[34] İ. Yanıkoğlu, B. L. Gorissen, and D. den Hertog, "A survey of adjustable robust optimization," *Eur. J. Oper. Res.*, vol. 277, no. 3, pp. 799–813, 2019.

[35] K. Margellos, P. Goulart, and J. Lygeros, "On the road between robust optimization and the scenario approach for chance constrained optimization problems," *IEEE Trans. Autom. Control*, vol. 59, no. 8, pp. 2258–2263, Aug. 2014.

[36] S. Bolognani and F. Dörfler, "Fast scenario-based decision making in unbalanced distribution networks," in *Proc. Power Syst. Comput. Conf. (PSCC)*, 2016, pp. 1–7.